ACS Synthetic Biology

Open Access
This article is licensed under CC-BY-NC-ND 4.0

pubs.acs.org/synthbio
Research Article

Toolbox of Characterized Genetic Parts for *Staphylococcus aureus*

Stephen N. Rondthaler, Biprodev Sarker, Nathaniel Howitz, Ishita Shah, and Lauren B. Andrews*

Cite This: *ACS Synth. Biol.* 2024, 13, 103−118
Read Online

ACCESS | Metrics & More | Article Recommendations | Supporting Information

ABSTRACT: *Staphylococcus aureus* is an important clinical bacterium prevalent in human-associated microbiomes and the cause of many diseases. However, *S. aureus* has been intractable to synthetic biology approaches due to limited characterized genetic parts for this nonmodel Gram-positive bacterium. Moreover, genetic manipulation of *S. aureus* has relied on cumbersome and inefficient cloning strategies. Here, we report the first standardized genetic parts toolbox for *S. aureus*, which includes characterized promoters, ribosome binding sites, terminators, and plasmid replicons from a variety of bacteria for precise control of gene expression. We established a standard relative expression unit (REU) for *S. aureus* using a plasmid reference and characterized genetic parts in standardized REUs using *S. aureus* ATCC 12600. We constructed promoter and terminator part plasmids that are compatible with an efficient Type IIS DNA assembly strategy to effectively build multipart DNA constructs. A library of 24 constitutive promoters was built and characterized in *S. aureus*, which showed a 380-fold activity range. This promoter library was also assayed in *Bacillus subtilis* (122-fold activity range) to demonstrate the transferability of the constitutive promoters between these Gram-positive bacteria. By applying an iterative design-build-test-learn cycle, we demonstrated the use of our toolbox for the rational design and engineering of a tetracycline sensor in *S. aureus* using the $P_{Xyl\text{-}TetO}$ aTc-inducible promoter that achieved 25.8-fold induction. This toolbox greatly expands the growing number of genetic parts for Gram-positive bacteria and will allow researchers to leverage synthetic biology approaches to study and engineer cellular processes in *S. aureus*.

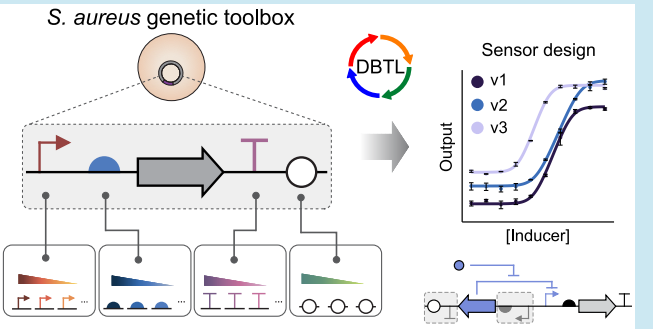

KEYWORDS: *biological parts, genetic standards, genetic toolbox, Gram-positive bacteria, characterized genetic elements*

INTRODUCTION

Staphylococcus aureus is an opportunistic Gram-positive pathogen and one of the most common causes of hospital-acquired infections[1] and biofilm infections.[2,3] Although it can colonize harmlessly on the skin or in the nose of healthy people, *S. aureus* can quickly alter its phenotype to cause deadly infections and target different organ systems of the body.[4] Its pathogenicity has been attributed to a combination of strong and pervasive cell attachment to a variety of implanted biomaterials[5,6] and tissues,[7] efficient aggregation and biofilm formation,[2] and the release of various toxins to evade the host immune response,[8] among other mechanisms. Due to these properties and the rapid rise of antibiotic resistant strains,[9,10] *S. aureus* is a bacterium of broad and critical interest for further study.

Despite its prevalence in biological and medical studies, *S. aureus* has been intractable to synthetic biology approaches and the precise control of gene expression. Most prior genetic studies in *S. aureus* have used allelic exchange,[11] gene deletion and complementation,[12,13] and random transposon mutagenesis[14] to interrogate gene function. Alternatively, synthetic biology can offer an efficient and faster investigation of cellular processes using genetic tools and synthetic DNA constructs. However, few studies have created fully synthetic DNA constructs in *S. aureus*, with most using large and imprecisely annotated DNA fragments from this organism to control gene expression.[15,16] Notably, these large DNA fragments can contain unidentified genetic regulatory elements, which can unexpectedly alter the gene expression. This makes it difficult to insert additional synthetic DNA or carefully tune expression due to the limited composability of the genetic parts and the challenges of cloning large DNA constructs.

As demonstrated in numerous other bacteria, standard and annotated genetic parts for *S. aureus* could enable easier and more efficient ways to engineer synthetic constructs. However, only few prior studies have implemented[17,18] or characterized such parts,[18,19] with none using a standard unit of measurement. Genetic part libraries have been created for various other microorganisms, such as *Escherichia coli*[20−22] and many other Gram-negative bacteria,[23−25] cyanobacteria,[26,27] and the model Gram-positive bacterium *Bacillus subtilis*.[28,29] Of note, genetic

Received: May 24, 2023
Revised: October 6, 2023
Accepted: October 10, 2023
Published: December 8, 2023

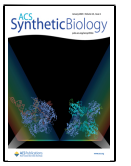

© 2023 The Authors. Published by American Chemical Society

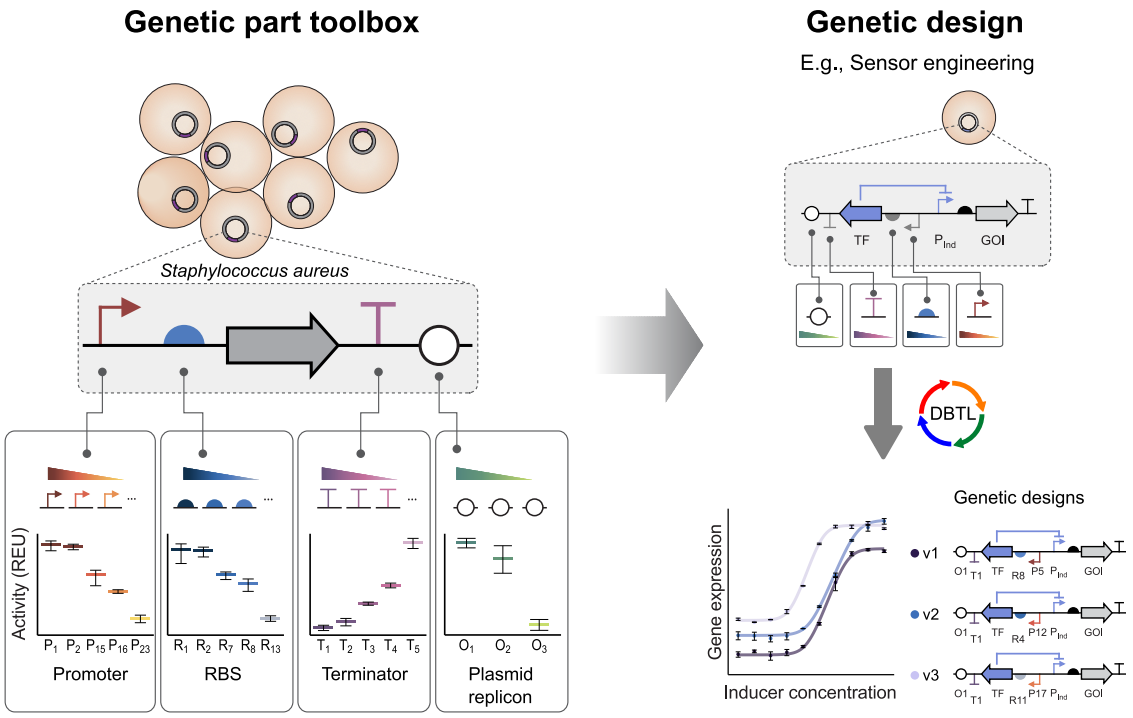

Figure 1. Overview of the *Staphylococcus aureus* genetic toolbox. (Left) Constitutive promoters, ribosome binding sites (RBSs), terminators, and plasmid replicons were characterized in standard relative expression units (REU) on plasmids in *S. aureus* to create the genetic parts toolbox. All parts were assayed using flow cytometry. (Right) These characterized parts can be used to rationally design the expression of synthetic genetic constructs in *S. aureus* for sensor engineering. The expression of the transcription factor (TF) of a sensor can be tuned using parts from the genetic toolbox and an iterative design-build-test-learn (DBTL) cycle to alter the expression of a gene of interest (GOI).

parts developed for Gram-positive bacteria have largely lagged behind those developed for Gram-negative bacteria. Large toolboxes of characterized genetic parts have greatly facilitated research and industrial applications in these microorganisms through the rational design of synthetic genetic constructs and the ability to fine-tune gene expression. Furthermore, standard DNA part toolboxes can allow researchers to build libraries of synthetic constructs with varying expression levels or large synthetic networks comprising many genes.[20,21,30] Creating large constructs using libraries of genetic parts with diverse sequences also decreases the risk of homologous recombination that could disrupt their function. Many physical sets of genetic parts[20,21,27] have been developed that can be directly used in one-pot Type IIS DNA assembly reactions[31−33] to quickly build synthetic multipart DNA constructs relative to traditional cloning methods, promoting the use of these toolboxes for synthetic biology applications.

In this study, we report a toolbox of standardized genetic parts for *S. aureus* (Figure 1), which is the first to date, to our knowledge. The genetic part plasmids incorporate orthogonal linker sequences for efficient Type IIS DNA assembly of synthetic constructs and easy exchange of different genetic parts to tune gene expression. Inspired by standards used in other bacteria,[28,34,35] we establish a standard relative expression unit (REU) for *S. aureus* using a whole plasmid reference, allowing standardized measurements of our genetic parts and direct comparison of gene expression under different conditions. Here, we characterize a variety of constitutive promoters, ribosome binding sites (RBSs), terminators, and plasmid replicons by using flow cytometry. The library of constitutive promoters shows a 380-fold range in activity and an average 1.35-fold difference in activity between the nearest promoters in strength, allowing for the fine-tuning of transcriptional expression of genes in synthetic constructs for *S. aureus*. Using these data, we uncover DNA sequence enrichment patterns for constitutive promoters of different strengths in *S. aureus*. Additionally, we reveal a high transferability of our constitutive promoter library between *S. aureus* and *B. subtilis*, observing a strong correlation between the promoter activity between these species. Thirteen RBSs derived from *B. subtilis* and a thermodynamic model[36−39] were characterized and demonstrated an 87.7-fold measurable range in expression, illustrating synthetic translational control of gene expression in *S. aureus*. Five Rho-independent terminators were measured and provided up to 95.3% reduction in gene expression for strong transcriptional insulation. Three plasmid replicons were assayed and displayed different characteristics for altering the gene expression. We demonstrate the application of our toolbox for rationally engineering synthetic DNA constructs in *S. aureus* by designing a tetracycline sensor for this bacterium. We created a tetracycline sensor using the $P_{Xyl\text{-}TetO}$ inducible promoter that displays low basal expression and 25.8-fold induction. Using this toolbox for *S. aureus*, researchers will be able to rationally design and build synthetic constructs for this nonmodel bacterium to investigate the function of native genes, express heterologous genes, and further develop synthetic biology tools.

RESULTS AND DISCUSSION

Design and Characterization of an *S. aureus* Genetic Toolbox. We aimed to create a standard genetic parts toolbox for *S. aureus* that would facilitate the efficient assembly of multipart synthetic DNA constructs. Thus, we first created a hierarchical Type IIS DNA assembly strategy for our physical

https://doi.org/10.1021/acssynbio.3c00325
ACS Synth. Biol. 2024, 13, 103−118

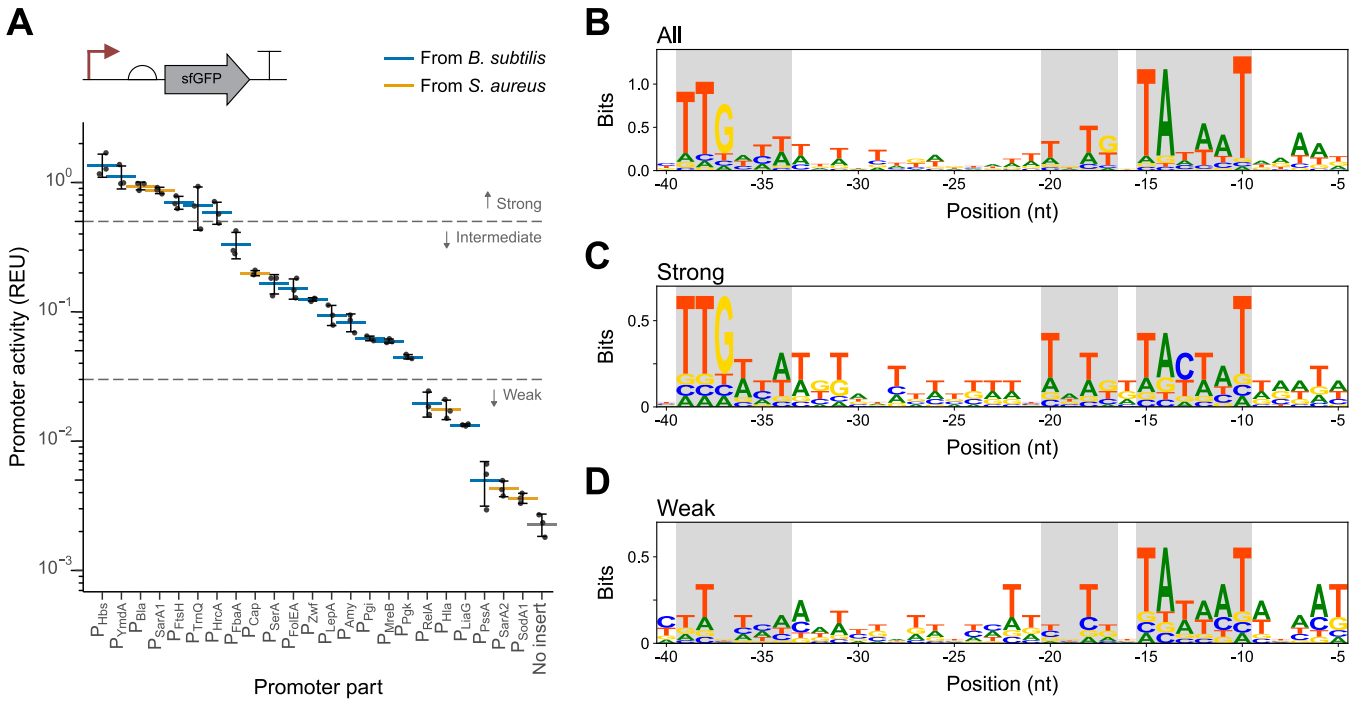

Figure 2. Constitutive promoter characterization in *S. aureus* ATCC 12600. (A) Different constitutive promoters originating from *B. subtilis* (blue) and *S. aureus* (orange) were inserted upstream of the RBS of *sfgfp* on a plasmid backbone containing the pC194 replicon. Single-cell fluorescence was measured by using flow cytometry and converted to relative expression units (REU) to determine promoter activity. Gray dashed lines indicate the REU breaks for each subset of promoters. (B–D) Information content sequence logos for (B) all, (C) strong, and (D) weak constitutive promoters were created from MAFFT alignments of trimmed promoter sequences (SI File 1) using the Python module Logomaker.[57] Locations of the −35, −16, and −10 constitutive promoter regions are indicated by gray highlights. All flow cytometry data are the average of three identical experiments performed on separate days ($n \geq 4000$ gated events per sample), with error bars showing 1 sample standard deviation above and below the mean.

S. aureus toolbox. We designed a set of 4-nucleotide orthogonal linker sequences[30] to assemble each type of the genetic part in the appropriate order (Table S1 and SI Extended Methods) and ensured all parts in this study did not contain a BbsI recognition site that would interfere with DNA assembly. An additional set of 3-nucleotide orthogonal linker sequences for the SapI restriction enzyme was created for the hierarchical assembly of entire transcription units into one of two destination vectors (pSR1000 and pSR1002). Transcription unit constructs were assembled on an intermediate plasmid using BbsI before subsequent assembly onto the destination vector using SapI.

We next established a relative expression unit (REU) in *S. aureus* using a reference plasmid (pCM29[15]) to standardize the measurement of each genetic part's activity. We chose this previously constructed plasmid as the reference due to its high constitutive expression of sfGFP and use in many other studies.[5,18,40] Specifically, pCM29 contains an *sfgfp* gene under high constitutive expression from the native upstream regulatory elements (i.e., promoter and RBS) of the *sarA* locus from *S. aureus*. Using this plasmid reference, arbitrary fluorescence units can be converted to REU relative to the fluorescence of pCM29, whose fluorescence we define as 1 REU (Methods). This reference standard is used to improve consistency in measurements between experiments under different conditions, such as dates, equipment, or laboratories, and facilitate the characterization of additional *S. aureus* genetic parts from other laboratories.[34,35] Each genetic part's activity was measured in REU using sfGFP output and flow cytometry analysis.

Constitutive Promoters from Gram-Positive Bacteria Show a Large Range in Activity and Transferability. We characterized 24 constitutive promoters in *S. aureus*, to control gene expression at the level of transcription. Several libraries of native gene promoter fragments have been characterized previously in *S. aureus*,[41,42] but these genetic parts have used large DNA fragments (>100 base pairs (bp)) that contain both a promoter and putative RBS. Thus, we aimed to characterize short promoters (<65 bp) to minimize the inclusion of unknown regulatory elements and for easier cloning of synthetic constructs. We chose 6 promoters from *S. aureus* used in previous studies[43−47] that include annotated promoter elements and no annotated transcription factor binding sites. Because few annotated *S. aureus* promoters are reported in the literature, we selected additional characterized constitutive promoters originating from *B. subtilis*, a well-studied Gram-positive bacterium with larger libraries of genetic parts. We chose 18 *B. subtilis* promoters from either genetic parts toolboxes[28,29,48] or studies with annotated promoter sequences.[49−55] We predicted that these constitutive promoters would function in *S. aureus* as other promoters originating from *B. subtilis* are functional in *S. aureus*,[19] and the two Gram-positive bacteria contain sigma A factors with significant homology between their protein sequences.[56] To measure the activity of each constitutive promoter in the library, the promoter upstream of *sfgfp* was replaced with the corresponding promoter part on the pCM29 plasmid backbone containing the pC194 replicon (Figure 2A).

In total, 23 constitutive promoters were assayed on pCM29 and spanned an activity range of 380-fold, with an average

https://doi.org/10.1021/acssynbio.3c00325
ACS Synth. Biol. 2024, 13, 103−118

1.35-fold change in activity between promoters of the nearest strength (Figure 2A). One additional constitutive promoter (P_{Veg}) was characterized on a lower copy number plasmid replicon (LAC-p01, Figure S1) due to an inability to transform the synthetic construct on the pC194 replicon into *S. aureus* (Supplemental Note 1). The promoters originating from *B. subtilis* and *S. aureus* spanned nearly the same range of activity in *S. aureus* (273-fold and 260-fold, respectively), demonstrating a high range of activity of the *B. subtilis* promoters in *S. aureus*. Constitutive promoters were also characterized with the ribozyme RiboJ between the promoter and RBS (Figure S2) to insulate the measured promoter activity from the effects of each promoter's RNA leader sequence, an important consideration in the design of many synthetic constructs such as genetic circuits.[58] RiboJ cleaves the RNA at a defined location, removing the upstream transcription start site sequence and leaving a constant sequence upstream of the RBS in the resulting mRNA transcript.[58] The results showed a strong linear correlation (R^2 = 0.96, Pearson's coefficient r = 0.94) between the promoter activity measured with and without RiboJ (Figure S2).

Next, we investigated whether the characterized promoters showed different sequence enrichment patterns, depending on their relative strengths. Consensus sequences for native *S. aureus* constitutive promoters have not been investigated, so we used the constitutive promoter consensus sequences from *B. subtilis*[49] (TTGACA, TRTG, and TATAAT for the −35, −16, and −10 regions, respectively) to evaluate the motifs from our constitutive promoter library. Using the MAFFT software,[59] we aligned the annotated or putative −35 and −10 sequences of the 23 constitutive promoters characterized on the pC194 replicon (Methods). The promoters were divided into subsets of strong (REU > 0.5, n = 7), intermediate (0.03 ≤ REU ≤ 0.5, n = 10), and weak (REU < 0.03, n = 6) strength, as indicated in Figure 2A. Information content sequence logos of the resulting alignments for all promoters and each subset showed different enrichment patterns of the major promoter regions (Figures 2 and S3).

As displayed in Figure 2B, the alignment of all characterized constitutive promoters showed the same −10 region consensus sequence as that for *B. subtilis* constitutive promoters (TATAAT) and slightly differing −35 and −16 sequences (TTGATT and TNTG, respectively, for our promoter library). This baseline sequence enrichment pattern provided a comparison for each promoter subset, but it is not necessarily indicative of enrichment patterns for natural *S. aureus* constitutive promoters since most characterized promoters in this study originated from *B. subtilis*. Interestingly, the strongest promoters we characterized in *S. aureus* showed the greatest enrichment of a different set of −35 and −10 region sequences than that of all characterized promoters but a similar −16 sequence (Figure 2C). This observation suggests that the strongest constitutive promoters in *S. aureus* may not necessarily contain all three promoter region consensus sequences, similar to previous findings in *B. subtilis* promoter engineering studies.[60,61] Alternatively, the weakest promoters showed relatively weak enrichment of −35 and −16 sequences that do not match those of the baseline but stronger enrichment of a −10 region that matches the baseline (Figure 2D). Promoters of intermediate strength showed an enrichment pattern that appeared to be a mixture of strong and weak promoters. Specifically, this pattern had much greater enrichment of a canonical TATAAT −10 motif compared to the strong promoters and also greater enrichment of a non-canonical −35 region compared to the weak promoters (Figure S3). Overall, the different enrichment patterns for our promoter subsets suggest complex interactions between promoter regions that control the activity of constitutive promoters in *S. aureus*.

Different sequence enrichment patterns were also seen when the promoters are grouped by species and strength (Figure S3). Constitutive promoters originating from *B. subtilis* showed enrichment similar to those observed for all promoters, likely because most promoters in our set originated from this bacterium. The *S. aureus* promoters, however, demonstrated slightly different enrichment sequences for each promoter region for both the strong/intermediate and weak promoters, especially in the sequence −16 sequence. This may suggest that promoters from *S. aureus* contain different native consensus sequences compared to those from *B. subtilis*, although *S. aureus* transcription machinery remains able to recognize *B. subtilis* promoter sequences (Figure 2A). However, a more thorough investigation of the native *S. aureus* constitutive promoter structure and sequences is required due to the very small number of native *S. aureus* promoters (n = 6) characterized in this study.

We compared the activities of the 24 constitutive promoters in *S. aureus* and *B. subtilis* to determine their transferability between these Gram-positive bacteria. We placed a constitutive promoter from the library upstream of *gfp* with the genetic insulator RiboJ (Figure S4), then integrated this synthetic construct at the *amyE* site on the genome of *B. subtilis* 168. The resulting promoter activity was measured using flow cytometry in relative promoter units (RPU) relative to a fluorescent reference construct (P_{FtsH}, RiboJ, RBS, *gfp*, and L3S2P21 terminator) integrated at the *amyE* site in *B. subtilis* for insulated expression of GFP (Methods). Excluding an outlier promoter (P_{SodA1}) that showed low fluorescence near the autofluorescence of the wildtype strain, the promoter activities measured in *B. subtilis* extended a range of 122-fold, with an average 1.26-fold change in activity between adjacent promoters of descending strength (Figure S4). This activity range was lower than that measured in *S. aureus* (380-fold) but with a comparable fold-change difference between promoters of the nearest strength (1.35-fold in *S. aureus*). Despite the difference in activity ranges, the promoter activities showed a strong linear correlation between the two species (Figure 3, R^2 = 0.894, r = 0.946), demonstrating high transferability of these constitutive promoter parts between similar Gram-positive species. Additionally, this suggests that other promoters characterized in *B. subtilis* may function similarly in *S. aureus*, providing a rich source of additional genetic parts for this bacterium.

Ribosome Binding Sites from *Bacillus subtilis* Allow Tunable Gene Expression in *S. aureus*. We assayed 13 RBSs in *S. aureus*, a common genetic element used to tune gene expression at the level of translation. Like constitutive promoters, few *S. aureus* RBS sequences have been reported in the literature,[18,43] and only one small set has been characterized.[18] This set of *S. aureus* RBSs exceeded 100 nucleotides from the promoter transcription start site, longer than RBSs typically used in synthetic biology. Ribosomes from Gram-positive bacteria have been shown to recognize RBSs from other Gram-positive species,[43] and the anti-Shine-Dalgarno sequences located at the 3′ region of the 16S rRNA genes from *S. aureus* and *B. subtilis* are identical (Figure

https://doi.org/10.1021/acssynbio.3c00325
ACS Synth. Biol. 2024, 13, 103−118

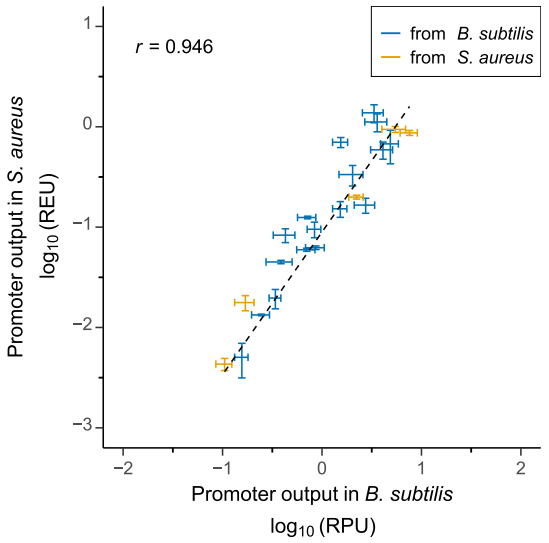

Figure 3. Comparison of constitutive promoter strengths between *S. aureus* and *B. subtilis*. The activities of constitutive promoters originating from *S. aureus* (orange) and *B. subtilis* (blue) from the promoter library in Figure 2A were measured using flow cytometry and converted to relative expression units (REU) in *S. aureus* and relative promoter units (RPU) in *B. subtilis*. P_{SodA1} was removed due to no significant activity in *B. subtilis*. Linear regression was performed on the $\log_{10}$ transformed data, and the resulting Pearson coefficient (r) is shown. All flow cytometry data are the average of three identical experiments performed on separate days ($n \geq 4000$ gated events per sample), with error bars showing 1 sample standard deviation above and below the mean.

S5). Therefore, we chose a set of short (<25 bp), well-characterized RBSs from *B. subtilis*[28] to characterize in *S. aureus*. We also created mutated versions of these natural RBSs via point mutations in the Shine-Dalgarno sequence and designed synthetic RBSs using a thermodynamic model (RBS Calculator)[36−39] to increase the number of RBSs. To measure the expression level of our RBS set, a constitutive promoter (moderately strong P_{Cap} or strong P_{SarA1}) and each RBS were inserted in front of *sfgfp* on a plasmid backbone containing the pC194 replicon (Figures 4A and S6A). Two constitutive promoters of different strengths were used to assay the RBSs to determine whether the promoter strength affected the measured RBS expression levels. We also assayed gene expression levels with the ribozyme RiboJ between the promoter and RBS to investigate the effect of RiboJ on RBS strength and insulate the RBS sequence from different promoter sequences (Figures 4B and S6B). We defined active RBSs in these data sets as those with expression levels greater than the measured activity of sfGFP on the same plasmid backbone without a constitutive promoter (0.00228 REU, Figure 2A). Note that some RBSs in combination with the P_{SarA1} promoter could not be assayed due to an inability to obtain *S. aureus* transformants after three electroporation attempts (Supplemental Note 1).

The active RBSs with P_{Cap} and without RiboJ spanned an 87.7-fold range in gene expression with a 2.4-fold average change for the nearest strength RBSs (Figure 4A). For comparison, active RBSs controlled by P_{SarA1} spanned only a 22.3-fold range in gene expression but had a similar average fold-change in activity (2.4-fold, Figure S6A). When RiboJ was included, the total range in gene expression for active RBSs with P_{Cap} decreased to 25.8-fold, and the average fold-change decreased to 1.6-fold for nearest strength RBSs (Figure 4B). Similarly, the active RBSs showed a lower range in the gene expression (13.5-fold) and a slightly smaller average fold-change in activity (1.6-fold) with P_{SarA1} and RiboJ compared to that without RiboJ (Figure S6B). As expected, the output was generally greater when expressed from the stronger P_{SarA1} promoter compared to the P_{Cap} promoter with and without RiboJ in the construct (4.0-fold with RiboJ and 5.6-fold without RiboJ, Figure S7), which is consistent with the measured promoter activity during promoter characterization

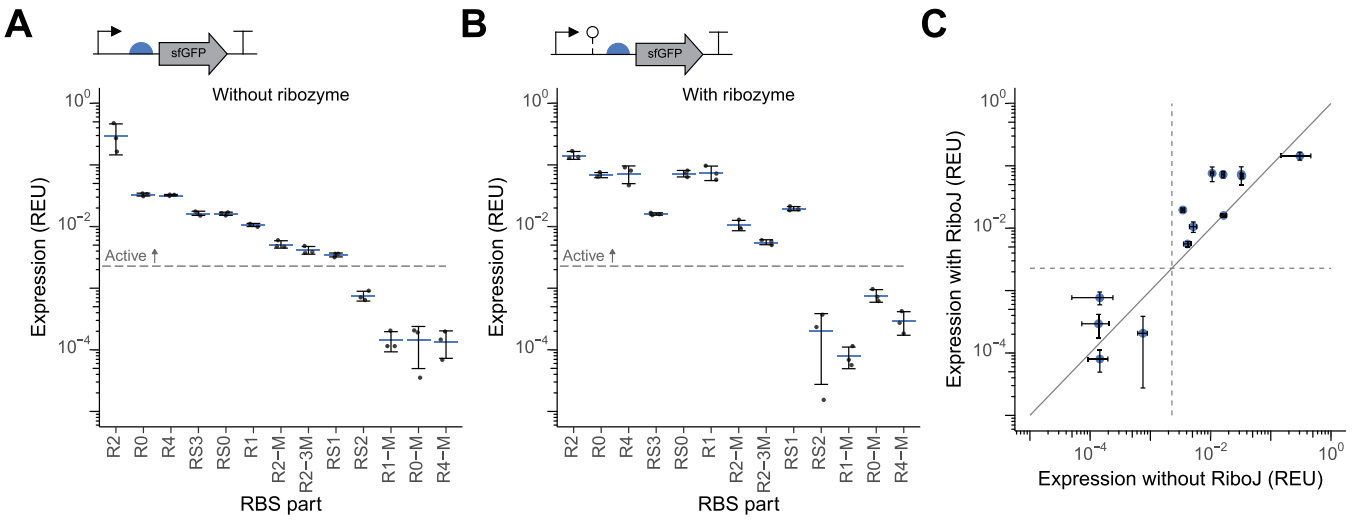

Figure 4. Ribosome binding site (RBS) characterization in *S. aureus* ATCC 12600. The moderately strong constitutive promoter P_{Cap} and different RBSs (A) without or (B) with the genetic insulator RiboJ were inserted upstream of *sfgfp* on a plasmid backbone containing the pC194 replicon. Single-cell fluorescence was measured using flow cytometry and converted to relative expression units (REU) to determine RBS expression. (C) Expression level for each RBS without RiboJ is plotted against the expression level with RiboJ. The gray solid line shows the 1:1 relationship ($y = x$) for comparison. The light gray dashed lines in all plots indicate the minimum expression level we defined for an active RBS (0.00228 REU). All flow cytometry data are the average of three identical experiments performed on separate days ($n \geq 4000$ gated events per sample), with error bars showing 1 sample standard deviation above and below the mean.

https://doi.org/10.1021/acssynbio.3c00325
ACS Synth. Biol. 2024, 13, 103−118

(4.4-fold, Figure 2A). Most RBSs showed higher expression levels with RiboJ (Figures 4C and S6C), indicating the importance of the upstream untranslated region (UTR) on the gene expression for a given RBS in *S. aureus* and following what has been reported in *E. coli*.[62] Despite this, gene expression with and without RiboJ for these RBSs showed a moderate to strong correlation for their rank order (Spearman's coefficient, ρ = 0.830 with P_{Cap} and ρ = 0.771 with P_{SarA1}, Figure S8), demonstrating that the relative activities of these RBSs are consistent with and without RiboJ for both promoters. The presence of RiboJ also increased the linear correlation in gene expression between the two constitutive promoters for the active RBSs (r = 0.784 without RiboJ to r = 0.874 with RiboJ, Figure S7). This suggests that RiboJ insulates the RBS strength from the effects of the upstream 5′ UTR sequence and may be beneficial for finely tuning gene expression in *S. aureus* when substituting promoter parts. Overall, these characterization data demonstrated effective tuning of gene expression through translational control by swapping the RBS, both with and without the ribozyme RiboJ. Additionally, these results demonstrated that *B. subtilis* RBSs can be functional in *S. aureus*, which can be a source of additional RBS sequences in future work.

Rho-Independent Terminators Provide Strong Reduction in Gene Expression. Next, we characterized terminator genetic parts in *S. aureus* to control termination of transcription, which provides transcriptional insulation and prevents readthrough in DNA constructs. Five short terminators (<65 nucleotides) were chosen from a collection of synthetic and natural terminators of varying strength that have been thoroughly characterized in Gram-negative *E. coli*.[63] Rho-independent terminators were selected here because they terminate expression via secondary structures in the mRNA, and thus, were expected to function with greater independence of the host organism than Rho-dependent terminators. To assay activity, the terminator was placed between constitutive promoter P_{Cap} and genetic insulator RiboJ upstream of *sfgfp* on a plasmid backbone containing the pC194 replicon (Figure 5). Terminator activity was calculated as the ratio of the fluorescence of this synthetic construct and the fluorescence of the same construct without the upstream terminator. We chose this approach to measure terminator activity as opposed to another method commonly used for terminator characterization in *E. coli* (Chen et al.[63] and Cambray et al.[64]) requiring two fluorescent protein reporters so that we could use the one fluorescent reporter protein in *S. aureus* with standardized units established in this toolbox.

All five terminators significantly reduced gene expression, with four of the five terminators reducing expression by over 90% (maximum 95.3% reduction with L3S2P11) and the weakest terminator (ECK120051401) reducing expression by 49.9% (Figures 5 and S9). Additionally, these five terminators preserved the same order of terminator strengths (ρ = 1.0) in *S. aureus* as in *E. coli*,[63] suggesting transferability of Rho-independent terminators between distant bacterial species. Overall, these results demonstrate that Rho-independent terminators characterized in *E. coli* can function effectively in *S. aureus* with similar relative strengths, which can provide an abundant source of terminators for this bacterium.

Different Plasmid Replicons Can Strongly Affect Gene Expression. Lastly, we characterized three plasmid backbones for *S. aureus* with different replicons. These replicons initiate rolling circle DNA replication and were

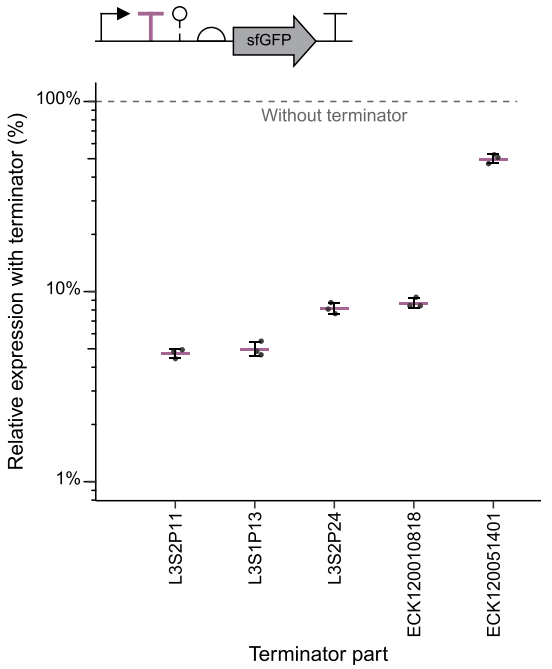

Figure 5. Terminator characterization in *S. aureus* ATCC 12600. Five Rho-independent terminators[63] were inserted between the moderately strong constitutive promoter P_{Cap} and genetic insulator RiboJ upstream of *sfgfp* on a plasmid backbone containing the pC194 replicon. Single-cell fluorescence was measured by using flow cytometry and converted to relative expression units (REU) to determine the resulting gene activity. Reduction in expression was calculated relative to the activity of the same synthetic construct without a terminator upstream of *sfgfp*. All flow cytometry data are the average of three identical experiments performed on separate days ($n \geq$ 4000 gated events per sample), with error bars showing 1 sample standard deviation above and below the mean.

chosen based on their use in prior studies and reported stability.[15,16,65] The pCM29[15] plasmid backbone used to characterize genetic parts here harbors the pC194 replicon and is reported to have a copy number of about 15 molecules per cell.[66] The pSR1000 plasmid backbone contains the pT181 replicon, which is reported to have a slightly higher copy number of approximately 20−25 molecules per cell.[16] Finally, the pSR1002 plasmid backbone contains the LAC-p01 replicon that has been shown to exhibit high stability over 100 generations and to be maintained at a copy number of about 5−10 molecules per cell.[65] To measure the activity of synthetic constructs in the genetic contexts of the pT181 and LAC-p01 plasmid replicons, we placed *sfgfp* genes expressed from five constitutive *S. aureus* promoters of varying strengths from our library on the plasmid backbones containing these replicons (Figure 6). These constitutive promoters were chosen to investigate if the relative expression between plasmid replicons was consistent with their expected copy numbers at different expression levels. To compare the data, the relative activities for each promoter were calculated relative to the average activity of the corresponding promoter construct on the backbone with the pC194 replicon.

The measured relative gene activities showed different expression patterns depending on the plasmid replicon (Figures 6 and S10). The pC194 and LAC-p01 plasmid replicons provided consistently higher and lower relative gene activities between the different constitutive promoters,

https://doi.org/10.1021/acssynbio.3c00325
ACS Synth. Biol. 2024, 13, 103−118

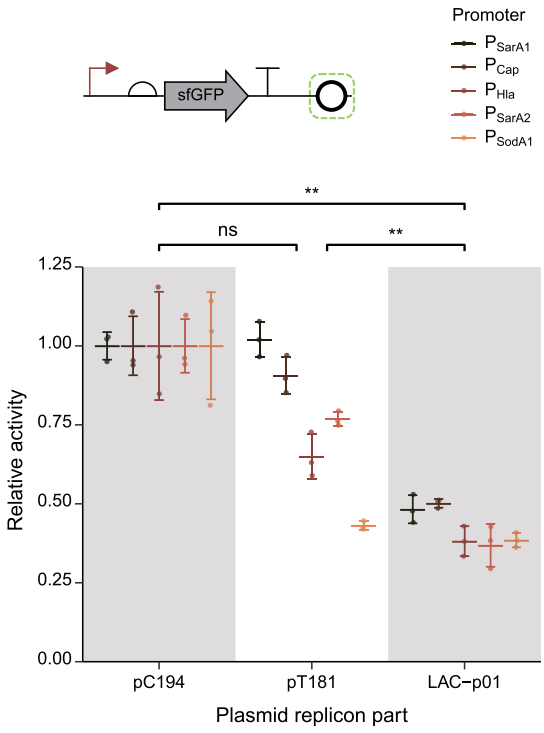

Figure 6. Plasmid replicon characterization in *S. aureus* ATCC 12600. Synthetic *sfgfp* genes with different *S. aureus* constitutive promoters of varying strengths were inserted onto plasmid backbones with different replicons. The resulting activity of each constitutive promoter was measured by using flow cytometry relative to the mean activity of the corresponding promoter characterized on the plasmid backbone containing the pC194 replicon. Asterisks indicate the results of a one-way nested ANOVA (plasmid replicon nested inside promoter) with Tukey posthoc analysis (ns: not significant, *: $p \leq 0.05$, **: $p \leq 0.01$). The adjusted *p*-values for the Tukey posthoc analysis are 0.999, 0.008, and 0.008 for the pC194/pT181, pC194/LAC-p01, and pT181/LAC-p01 pairs, respectively. All flow cytometry data are the average of three identical experiments performed on separate days ($n \geq 4000$ gated events per sample), with error bars showing 1 sample standard deviation above and below the mean.

respectively, unlike the pT181 replicon, which showed both lower and higher relative activities depending on the promoter tested. At the same time, both the pT181 and LAC-p01 replicons demonstrated more consistent relative activity measurements (i.e., smaller standard deviations) compared to the pC194 replicon for most promoters. When comparing relative activities for all synthetic constructs between plasmid replicons, only LAC-p01 showed significantly lower activity compared to the activities from the other two plasmid replicons ($p \leq 0.05$ for both, Figure 6). In contrast, the pC194 and pT181 replicons showed no statistical difference from this analysis. In this experiment, the relative expression levels for the pC194 and LAC-p01 replicons were generally consistent with their copy numbers as reported in the literature,[15,65] while the pT181 replicon showed greater variability and lower expression than expected based on its reported copy number.[16] We also measured the plasmid copy number by quantitative PCR for the subset of plasmids expressing sfGFP with P_{SarA1} (strong) or P_{Hla} (weak) promoters for all three replicons (SI Extended Methods, Figure S11). Interestingly, the measured copy number for the plasmids with the LAC-p01 replicon (36 ± 4 and 13 ± 3 copies per chromosome, respectively) and pC194 replicon (60 ± 40 and 25 ± 3 copies per chromosome, respectively) were greater than those previously reported,[15,65] while the measured copy number of the pT181 replicon (25 ± 3 and 9 ± 2 copies per chromosome, respectively) is in agreement with previous work.[16] However, only pT181 had a significantly lower measured copy number than did pC194 ($p \leq 0.05$, Figure S11), and very high variability was observed for the samples with the pC194 replicon and P_{SarA1} promoter in this experiment. Altogether, our results demonstrate that the expression of synthetic constructs in *S. aureus* depends on the choice of plasmid replicon, which is an important consideration for genetic design.

***S. aureus* Genetic Parts Toolbox Can Be Used To Create and Rationally Tune Sensors.** With this set of characterized genetic parts, we next sought to demonstrate the use of our toolbox to rationally design synthetic constructs of genetically encoded sensors in *S. aureus*. These small molecule sensors were encoded using inducible promoters and transcription factor proteins, which allosterically regulate the promoter activity via exogenous addition of the inducer. The transcriptional response of these sensors can be tuned by varying the expression of the allosteric transcription factor.[67,68] $P_{Xyl\text{-}TetO}$ has been previously used in *S. aureus* as a tetracycline or anhydrotetracycline (aTc) sensor using the TetR repressor.[19,69,70] This hybrid inducible promoter is composed of the P_{Xyl} promoter from *B. subtilis* with the consensus −35 and −10 promoter sequences for *B. subtilis* and the *tet* operator sequence from *E. coli* inserted between the −35 and −10 regions.[69] However, this sensor has shown high basal expression[19] and low dynamic range (<20-fold)[70,71] in *S. aureus*. Therefore, we aimed to tune the sensor's response by changing the constitutive promoter and RBS expressing *tetR* (Figure 7A), with the goal of increasing the sensor's dynamic range while maintaining low basal expression. Each sensor design's response was experimentally assayed by adding aTc to the growth media and measuring the resulting cell fluorescence via sfGFP. We used an iterative design-build-test-learn cycle to modify the sensor design based on the previous designs' characteristics.

Three active tetracycline sensor designs were characterized to increase the dynamic range of the sensor while keeping basal expression and cellular toxicity low in the final design (Figure 7 and Table S2). The first design (v1), constructed on a plasmid containing the pC194 replicon, showed 18.3-fold induction with basal and maximal expressions of 0.0044 and 0.080 REU, respectively (Figure 7). However, significant growth toxicity was observed during the assay, and the specific growth rate quantified by growth assays was significantly lower than that of the wildtype (Figures S12 and S13 and Table S3), suggesting that TetR was expressed too highly. Additionally, bimodal distributions in cell fluorescence were observed by flow cytometry (Figure 7C). Therefore, we devised more sensor designs using genetic parts with weaker activities, including the low copy number LAC-p01 replicon. Initially, a sensor design was constructed and characterized that showed constitutively high expression even with the addition of aTc (Figure S14 and Table S3), suggesting that TetR was not expressed enough. Thus, stronger constitutive promoters and RBSs were incorporated in additional sensor designs in later iterative design cycles. The second active tetracycline sensor design (v2) was constructed in the next iteration and displayed only 4.5-fold induction and an activity range from 0.019 to 0.084 REU (Figure 7). Although no significant cellular toxicity was

https://doi.org/10.1021/acssynbio.3c00325
ACS Synth. Biol. 2024, 13, 103−118

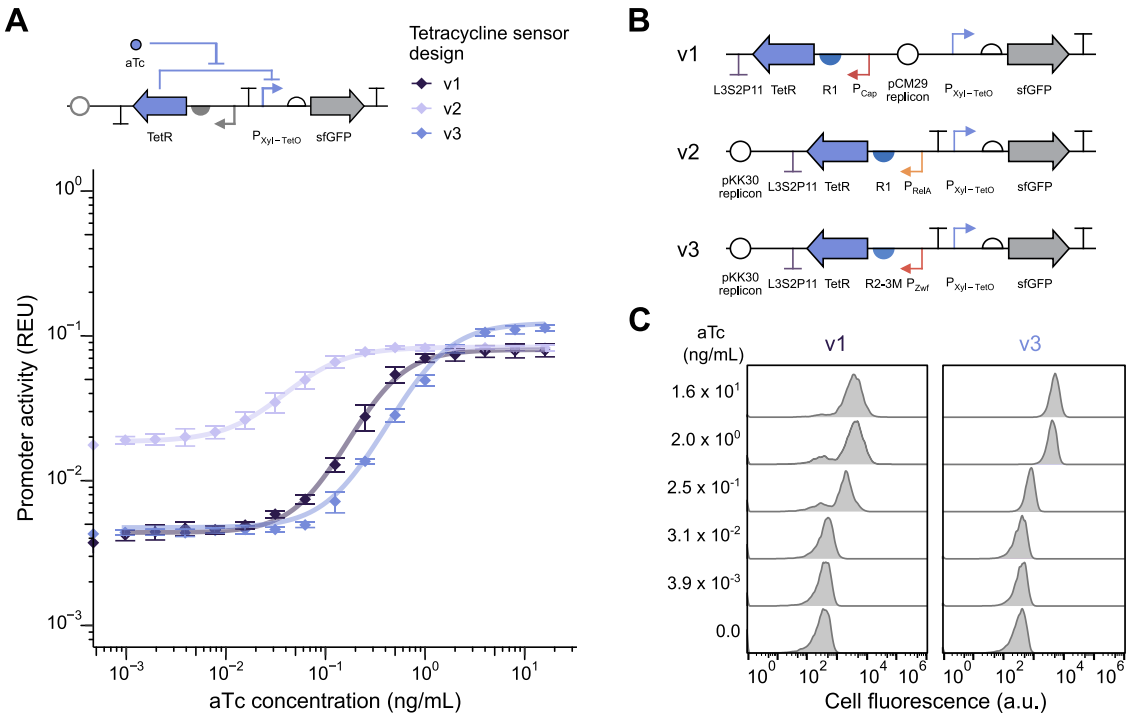

Figure 7. Rational design and tuning of a tetracycline sensor in *S. aureus* ATCC 12600. (A) Different designs of a tetracycline sensor using the $P_{Xyl\text{-}TetO}$ inducible promoter were designed and built using genetic parts characterized in the toolbox (gray parts) to tune the expression of the transcription factor TetR. The *sfgfp* gene was expressed from $P_{Xyl\text{-}TetO}$ to assess promoter activity. The response of each sensor design was quantified by titrating anhydrotetracycline (aTc), measuring single-cell fluorescence using flow cytometry ($n \geq 4000$ cell events per sample), and converting the fluorescence to relative expression units (REU) to determine promoter activity. Identical experiments were performed on 3 different days. The mean ±1 standard deviation is plotted. The response function (line) for each tetracycline sensor design was determined by fitting the experimental data to the Hill equation (Methods). (B) Genetic schematics depicting the genetic parts used for each tetracycline sensor design are shown. (C) Representative normalized histograms of cell fluorescence in arbitrary units (au) are given for the tetracycline sensors v1 and v3 with different concentrations of aTc.

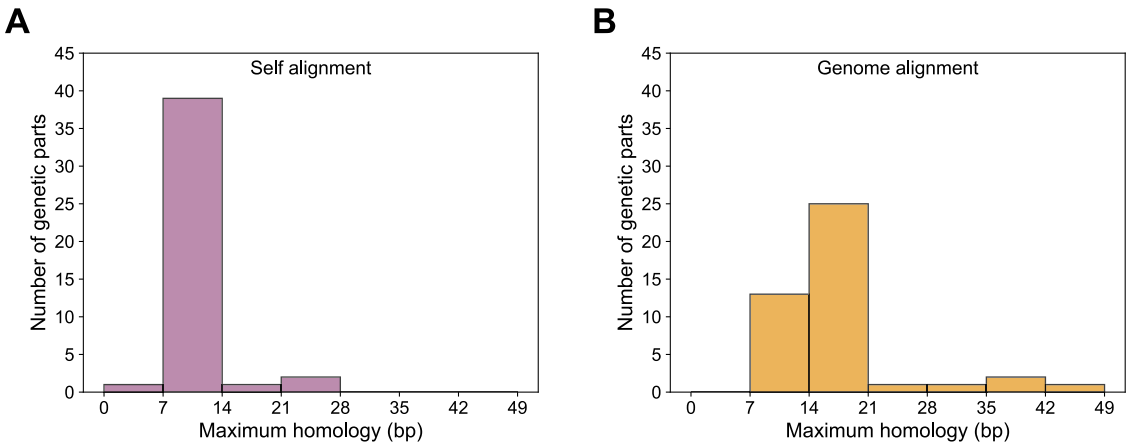

Figure 8. Maximum contiguous homology of the genetic parts in the toolbox with each other and the *S. aureus* ATCC 12600 genome. A total of 25 promoter, 13 RBS, and 5 terminator parts in the *S. aureus* toolbox (all parts except for the plasmid replicons and the P_{Spac} promoters) were BLAST-aligned against (A) each other and (B) the ATCC 12600 genome using options for short sequence alignments (SI Extended Methods). The maximum lengths of the alignments without mismatches in base pairs (bp) from the BLAST results were binned in 7 bp increments (inclusive of the lower increment) for display in histograms. The bin size was chosen as the minimum length of alignment detected by using BLAST. Histograms for the BLAST alignments with mismatches are given in Figure S17.

observed during the experimental assay, the dynamic range of tetracycline sensor v2 was greatly reduced compared to that of v1. Thus, we constructed and characterized a third design (v3), which displayed 25.8-fold induction spanning from 0.0047 REU and 0.12 REU without significant growth toxicity compared to the wild-type strain (Figure S12 and Table S3). Additionally, histograms of cell fluorescence for the tetracycline sensor v3 design showed a unimodal distribution (Figure 7C). The v3 tetracycline sensor design showed greater or comparable induction to previous tetracycline sensors characterized in *S. aureus*,[69−71] although basal and maximal expression levels cannot be directly compared due to different assays and experimental conditions. Attempts were made to engineer an isopropyl *β*-D-1-thiogalactopyranoside (IPTG)

https://doi.org/10.1021/acssynbio.3c00325
ACS Synth. Biol. 2024, 13, 103−118

sensor containing the P_{Spac} promoter using promoter engineering and the same approach used for the tetracycline sensor, but no designed sensor showed greater than 3-fold induction (Supplemental Note 2, Figures S15 and S16). Altogether, the design and characterization of tetracycline sensor v3 through our iterative approach demonstrate the use of the genetic parts toolbox to tune a genetically encoded sensor in *S. aureus*.

Genetic Parts Share Little Homology with Each Other and the *S. aureus* Genome. Homologous recombination between repetitive DNA sequences in the parts or host genome can lead to the failure of synthetic constructs.[72] For example, this can occur at low rates with as little as 23 base pairs of homology in *E. coli*, with increasing rates of recombination for greater lengths of homology and significantly decreasing rates by the inclusion of mismatches.[73] Therefore, to investigate the homology of our genetic parts in *S. aureus*, we aligned the sequences of all parts except the plasmid replicons and the P_{Spac} promoters to each other and the *S. aureus* ATCC 12600 genome using BLAST optimized for aligning short, repetitive sequences (SI Extended Methods). We then grouped the results into alignments without mismatches (contiguous homology, Figure 8) and alignments with mismatches (noncontiguous homology, Figure S17). The maximum alignment length with and without mismatches for all aligned parts is listed in SI File 1.

Histograms of each BLAST alignment without and with mismatches indicated that most parts share little homology with others in the toolbox and with the *S. aureus* ATCC 12600 genome (Figures 8 and S17). Most parts in the genetic toolbox (91%) showed fewer than 14 bp of continuous homology with each other (Figure 8A). In comparison, the parts showed greater contiguous homology against the ATCC 12600 genome, as only 30% of parts have fewer than 14 bp of homology (Figure 8B). However, 93% of aligned parts have less than 23 bp of contiguous homology with the genome, and all having less than 50 bp of homology. The parts with the greatest homology to the ATCC 12600 genome included four constitutive promoters originating from *S. aureus* (P_{SarA1}, P_{SarA2}, P_{SodA1}, and P_{Hla}). When considering mismatches in the BLAST alignments against each part, most parts displayed less than or similar noncontiguous homology to contiguous homology (Figure S17A), except for the pairs of the natural and mutated *B. subtilis* RBSs. Conversely, many parts showed greater noncontiguous homology against the ATCC 12600 genome, especially the constitutive promoters (Figure S17B). Overall, these BLAST alignment results demonstrate that 91% of the genetic parts in our toolbox share less than 30 bp of contiguous and noncontiguous homology with other parts and the *S. aureus* ATCC 12600 genome.

DISCUSSION

We have developed the first standardized genetic parts toolbox for *S. aureus*, including 24 constitutive promoters, 13 RBSs, 5 Rho-independent terminators, and 3 plasmid replicons. Our library of constitutive promoters showed 380-fold range of activity, notably much greater than a recent report of 20 constitutive promoters with high expression characterized in *S. aureus* (36-fold range).[42] Our promoters are also shorter than those from this previous library, which contains promoter parts of similar sizes to those traditionally used in this bacterium (Figure S18). Compared to genetic part toolboxes for *B. subtilis*, the activity range of our promoter set is similar to that of promoter libraries assayed in this model organism that showed 70.7-fold to 857-fold ranges in activity.[28] In addition, our RBS library showed a greater activity range (87.7-fold without RiboJ) than a previous set of RBSs measured in *S. aureus* (about 3-fold)[18] while also using shorter UTR sequences. The RBS library in our toolbox showed activity within an order of magnitude of RBS libraries measured in *B. subtilis* (11.5-fold to 313-fold).[28] Finally, we measured the effect of different terminators and plasmid replicons on gene expression in *S. aureus*. Altogether, our genetic toolbox contains a variety of genetic parts with ranges of strengths larger than those previously assayed in *S. aureus* and comparable to many established in *B. subtilis*, providing a strong foundation for the development of synthetic constructs in *S. aureus*.

By establishing the standard REU measurement and assaying a variety of parts in the REU, additional genetic parts can be added to the toolbox. These parts could be chosen and measured individually, such as in this work, or created and screened using high-throughput techniques from synthetic biology. For example, saturation or random mutagenesis could be performed on genetic parts in the toolbox, then combined with a high-throughput screening technique (i.e., sort-seq) to create larger part libraries for *S. aureus*. Furthermore, computer models and designs have also been established to aid in the design of fully synthetic genetic parts,[36,74,75] which may be used to create genetic parts with greater sequence variation than other synthetic biology techniques. These methods to create or expand genetic parts libraries have been applied in other bacteria, including *E. coli*[74−77] and *B. subtilis*[28] as well as some nonmodel bacteria such as *Corynebacterium glutamicum*.[78]

We revealed that many genetic parts are transferable to *S. aureus* from different bacterial species. While several promoter parts originating from *B. subtilis* are functional in *S. aureus* (such as $P_{Xyl\text{-}TetO}$[79] and P_{Spac}[80]), studies have not compared relative strengths of constitutive promoters between these two species. Interestingly, our constitutive promoter library showed high transferability between these related Gram-positive bacteria, despite assaying the parts in different genetic contexts (i.e., plasmid-based for *S. aureus* and chromosomally integrated for *B. subtilis*). Notably, five of the six constitutive promoters from *S. aureus* had significant activity in *B. subtilis*, with the promoter that had nonsignificant activity (P_{SodA1}) in *B. subtilis* showing very low activity in *S. aureus*. This transferability of promoters may be due to similarities of the sigma A factors between *S. aureus* and *B. subtilis*.[56] Additionally, the natural RBSs originating from *B. subtilis* (*R*0, *R*1, *R*2, and *R*4) were functional in *S. aureus*. The transferability of these promoters and RBSs between *B. subtilis* and *S. aureus* is noteworthy considering the different genomic GC contents of these bacteria (44% and 33%, respectively). Interestingly, a previous study investigated the transferability of natural promoters and RBSs originating from a variety of bacteria between *E. coli*, *B. subtilis*, and *Pseudomonas putida*, uncovering that many regulatory regions were species-specific, some universal, and others functional only in closely related species (i.e., *E. coli* and *P. putida*).[81] Rho-independent terminators originating from Gram-negative *E. coli* were also transferable to *S. aureus*, and all five characterized terminators showed the same order of terminator strengths between the species. To the best of our knowledge, this is the first report demonstrating the characterization of terminators from Gram-negative bacteria in *S. aureus*. The transferability of these heterologous promoters, RBSs, and

https://doi.org/10.1021/acssynbio.3c00325
ACS Synth. Biol. 2024, 13, 103−118

terminators to *S. aureus* not only provides additional potential sources of genetic parts for this nonmodel bacteria but also may inspire further investigation of the transferability of specific genetic parts between Gram-positive and more diverse bacteria.

The genetic parts in our toolbox were assayed on multicopy plasmids for easier construction of synthetic designs, faster characterization, and detection of weak genetic parts that may not be measurable when expressed from the chromosome. The use of plasmid-based gene expression could come at the cost of greater metabolic burden to the cells, yet only one of eight different plasmid constructs assayed showed significantly lower ($p < 0.05$) growth rate compared to the wild type in growth assays (Figure S12 and Table S3). However, we were unable to transform *S. aureus* with some of the RBS characterization plasmids that included the strong constitutive promoter P_{SarA1}, possibly due to the higher copy number of the pC194 replicon causing an increased metabolic burden (Supplemental Note 1). Integration on the chromosome can be used to reduce the copy number and, thus, the metabolic burden of a synthetic construct. However, methods to integrate synthetic DNA constructs onto the genome in *S. aureus* are generally time-consuming and have low efficiency.[11,82,83] The plasmid replicons characterized here employ the rolling circle mode of replication, which can show reduced genetic stability as the size of the plasmid increases.[84] Alternatively, plasmids that use the theta mode of replication (e.g., pSK1[70,85] and pSK41[70]) are maintained at lower copy numbers and are reported to be more genetically stable.[85,86]

We developed our *S. aureus* genetic parts toolbox using standard parts and a standardized method, allowing other researchers to apply and expand the *S. aureus* toolbox. The hierarchical Type IIS DNA assembly strategy will facilitate the design and assembly of custom synthetic plasmids to express genes of interest in *S. aureus* for a variety of applications such as studying putative antibiotic resistance genes or tuning the expression of genomic tools. Our standardized REU measurement allows other researchers to directly compare and add parts to the toolbox. Altogether, our toolbox introduces standard genetic parts for the rational design and efficient construction of synthetic DNA constructs in *S. aureus*, establishing a powerful foundation for synthetic biology techniques to study the cellular processes of this nonmodel, pathogenic organism.

METHODS

Strains and Plasmids. *Staphylococcus aureus* ATCC 12600 (BEI resources) was used to characterize all genetic parts. *Bacillus subtilis* 168 was used to characterize the constitutive promoters in this species. All cloning was performed in *Escherichia coli* NEB 5-alpha (New England BioLabs, NEB), NEB 10-beta (NEB), or IM08B.[87] All *S. aureus* plasmid constructs used to characterize genetic parts were transformed into strain IM08B, which contains the enzyme methylation system of ATCC 12600, before transformation into ATCC 12600 for characterization. Plasmid names and descriptions are listed in Table S4, with additional details in SI File 1. Plasmid maps of the REU and RPU reference plasmids (pCM29 and pNH446, respectively) and the *S. aureus* plasmid backbones pSR1000 and pSR1002 are given in Figure S19. Representative maps of the characterization plasmids are shown in Figure S20. The DNA sequences for each genetic part are listed in Table S5, with additional information in SI File 1. All DNA primers and oligomers were synthesized by Integrated DNA Technologies (IDT) and are listed in Table S6. All genetic parts in this work are provided in the SBOL format in SI File 2. The LAC-p01 replicon plasmid without a synthetic insert and select constitutive promoter characterization plasmids are available through Addgene.

Media and Reagents. See the SI extended methods for all media recipes. *E. coli* and *B. subtilis* strains were cultured in Luria−Bertani (LB) broth (Fisher Bioreagents) and on LB agar plates with antibiotics supplemented as necessary. *S. aureus* strains were grown in Tryptic Soy Broth (TSB) and tryptic soy agar for culturing and SSM9PR minimal media[88] for assaying genetic part activities, with antibiotics supplemented as necessary. *B. subtilis* strains were grown in M9 media supplemented with 20 μg/mL tryptophan for measuring the activity of the constitutive promoters. For transformations, *E. coli* and *B. subtilis* strains were recovered in Super Optimal Broth with Catabolite repression (SOC) and *S. aureus* strains were recovered in B2 recovery media.[89] For culturing *E. coli* strains, the following concentrations of antibiotics (all from GoldBio) were used to maintain plasmids as needed−ampicillin/carbenicillin, 100 μg/mL; erythromycin, 300 μg/mL for liquid media or 300−400 μg/mL for solid media; kanamycin, 50 μg/mL. For culturing *S. aureus* strains, the following concentrations of antibiotics were used as needed−chloramphenicol, 10 μg/mL: erythromycin, 10 μg/mL. For culturing *B. subtilis* strains, chloramphenicol was used at 5 μg/mL as needed. For assaying the response functions of the genetically encoded sensors, anhydrotetracycline (aTc; Sigma-Aldrich) and isopropyl β-D-1-thiogalactopyranoside (IPTG; GoldBio) were used for the tetracycline and IPTG sensors, respectively.

DNA Construction. Detailed notes on constructing all plasmids to characterize each type of genetic part are given in Supplemental Note 3. All cloning was done in *E. coli* prior to electroporation into *S. aureus* ATCC 12600 for measurement. See the SI Extended Methods for detailed procedures for cloning techniques. Briefly, all PCRs were performed using Q5 high fidelity polymerase (NEB) according to the manufacturer's protocol for most conditions. Promoters were created by annealing DNA oligos or were otherwise PCR amplified from plasmids or *B. subtilis* 168 genomic DNA. RBSs were inserted in front of *sfgfp* via amplification of the plasmid backbone by adding the RBS to the 5′ end of a primer. All terminators were created by annealing DNA oligos. DNA fragments were purified using the GenCatch PCR Purification Kit according to the manufacturer's protocol. Plasmid DNA minipreps were performed using the QIAprep Spin Miniprep Kit according to the manufacturer's protocol. All synthetic plasmids were assembled using Type IIS DNA assemblies with custom orthogonal linker sequences[30] (Table S1). After assembling and transforming a plasmid into *E. coli*, colonies were screened using colony PCR, and then, a single positive colony was grown overnight and the plasmid DNA purified. All assembled synthetic genes were verified using Sangar sequencing (Genewiz, Azenta Life Sciences).

Transformation of *E. coli*. Chemical transformation was used to introduce DNA constructs into *E. coli* strains for cloning, although some plasmids were introduced using electroporation for greater efficiency (SI Extended Methods). For chemical transformation, aliquots of chemically competent cells (5−50 μL for IM08C, 5 μL for NEB 5-alpha and NEB 10-beta) were thawed on ice. Chemically competent NEB 5-alpha

https://doi.org/10.1021/acssynbio.3c00325
ACS Synth. Biol. 2024, 13, 103−118

and NEB 10-beta cells were purchased from NEB while chemically competent IM08B cells were prepared in-house (SI Extended Methods). DNA was then added to each aliquot at a ratio of up to 1 μL of DNA assembly reaction mixture per 5 μL of cells or at least 100 ng of purified plasmid DNA. The cell mixture was incubated on ice for 30 min before heat shock on a thermocycler at 42 °C for 30 s, then incubated on ice again for 2−5 min. SOC recovery media was added to each aliquot at a ratio of 95 μL of SOC per 5 μL of cells, and the cells were incubated in a shaking incubator at 37 °C, 250 rpm for 60 min to recover. The cells were then spread on an LB agar plate with appropriate antibiotics and incubated overnight at 37 °C.

Electrocompetent Cell Preparation for *S. aureus*. Electroporation was used to introduce synthetic plasmids into *S. aureus* ATCC 12600. To prepare the cells for electroporation, a tryptic soy agar plate was streaked with ATCC 12600 and grown overnight at 37 °C. A single colony was used to inoculate 1−2 mL of TSB media and grown overnight in a shaking incubator at 37 °C and 250 rpm. The overnight culture was used to inoculate 101 mL of fresh TSB to an OD_{600} of 0.01 A in a 250 mL Erlenmeyer flask. The cells were grown at 37 °C and 250 rpm in a shaking incubator to the exponential phase, defined as an OD_{600} of 0.45−0.55 A. The cells were then transferred to 50 mL conical centrifuge tubes (Falcon or Genesee Scientific) to chill in an ice−water bath for 10 min to slow growth. All subsequent steps were performed on ice. The conical tubes were centrifuged at 8000 g and 4 °C for 10 min (Eppendorf Centrifuge 5810 R) to pellet the cells. The supernatant was removed by decanting, and the cell pellet gently was resuspended in 50 mL of ice-cold sterile Milli-Q water. The cell mixture was chilled in the ice−water bath for 3−5 min before centrifugation under the same conditions to wash the cells. These wash steps (removing the supernatant, resuspending, chilling, and centrifuging) were performed twice more, resuspending the cells in 25 mL of ice-cold sterile Milli-Q water and then 12.5 mL of sterile 10% (v/v) glycerol for each wash. After the final centrifugation, the cells were gently resuspended in 500 μL ice-cold sterile 10% glycerol and then divided into 100 μL aliquots for electroporation immediately (for the best transformation efficiency) or stored at −70 °C.

Electroporation of *S. aureus*. To electroporate DNA into *S. aureus*, 100 μL aliquots of electrocompetent cells were thawed on ice, and ≥1000 ng of plasmid DNA extracted from IM08B was added. Cell mixtures were incubated on ice for 30 min before 100 μL of the cell-DNA mixture was added to chilled 1 mm electroporation cuvettes (Fisher Scientific) and electroporated using a MicroPulser Electroporator (Bio-Rad) at a voltage of 2.1 kV and a time constant of 1.1 ms.[90] B2 recovery media (500 μL) prewarmed to 37 °C was immediately pipetted into the cuvette and used to mix the cells before transferring to a 1.5 mL microfuge tube. Samples were incubated for 1 h at 37 °C and 250 rpm in a shaking incubator to recover. If needed, samples were concentrated before plating by centrifuging for 5 min at 15,000*g* and room temperature, removing some volume supernatant by pipetting, and resuspending the cells in the remaining supernatant. The cells were then plated on a tryptic soy agar plate with the appropriate antibiotic and grown overnight at 37 °C.

Competent Cell Preparation for *B. subtilis* 168. A colony from a streaked plate of *B. subtilis* 168 was grown overnight in a shaking incubator at 37 °C and 250 rpm. Next, the overnight culture was used to inoculate 12.5 mL of prewarmed nutrient-rich SpC media in a 125 mL Erlenmeyer flask to an initial OD_{600} of 0.01 A. The culture was then incubated in a shaking incubator at 250 rpm and 37 °C and the OD_{600} was taken every 30 min to measure a growth curve. After reaching the start of the stationary phase (as determined through the R^2 for a line of best fit during exponential growth), the culture was grown two more hours to increase the yield of cells. The culture was diluted 10-fold with prewarmed starvation media SpII, then incubated in the shaking incubator at 250 rpm and 37 °C for 90 min. The cells were harvested at room temperature through centrifugation, and then some of the supernatant was removed and the cells concentrated 20-fold in the remaining SpII media. Competent cells were stored in 10% glycerol at −70 °C.

Transformation of *B. subtilis* 168. The *B. subtilis* chromosomal integration plasmids containing the synthetic construct to characterize the constitutive promoters were first linearized using BsaI-HF v2 (NEB). Approximately 1 μg of linearized DNA was added to 100 μL of competent *B. subtilis* cells in a culture tube and incubated in a shaking incubator at 250 rpm and 37 °C for 1 h. SOC recovery media (500 μL) was then added, and the cells were incubated under the same conditions for 2 h to recover. The samples were then concentrated 5-fold by pelleting cells through centrifugation, removing excess supernatant, and resuspending in the remaining supernatant before plating on LB agar plates with chloramphenicol.

Flow Cytometry Assay for Genetic Part Characterization. All genetic parts were assayed under the exponential growth phase using flow cytometry as follows. *S. aureus* ATCC 12600 strains containing the different synthetic plasmids for genetic part characterization and the negative control (wild-type) and positive control (containing the pCM29 reference plasmid) strains were streaked on tryptic soy agar plates with the appropriate antibiotic and grown overnight at 37 °C. Single colonies were used to inoculate 200 μL of SSM9PR, with antibiotics as needed, in a 96-well U-bottom plate (Costar) and covered with an Aeraseal (Excel Scientific). The samples were grown in a plate-shaking incubator (ELMI SkyLine DTS-4 Shaker) at 37 °C and 1000 rpm for 16 h. Samples were then diluted 44.4-fold (30 μL of sample media into 170 μL of fresh media, twice) into SSM9PR media with antibiotics as needed and grown for 3 h under the same growth conditions. After this initial growth, samples were diluted 96.7-fold (30 μL of sample media into 170 μL of fresh media, then 10 μL of diluted sample media into 145 μL of fresh media) into SSM9PR media with antibiotics and chemical inducers as needed. The samples were grown for an additional 5 h under the same growth conditions. Next, the *S. aureus* samples were fixed using 4% paraformaldehyde in phosphate buffered saline (PBS) as described below. Cells were diluted into PBS with 2 mg/mL kanamycin prior to flow cytometry with the goal of approximately 800−1,200 gated events/s. The fluorescence of each sample was measured using an Accuri C6 Flow Cytometer (BD Biosciences) at a slow flow rate using the FL1-A channel. The thresholds of either 25,000 for the FSC-H channel or 27,000 for the FSC-H channel and 1250 for the SSC-H channel were used to decrease noise in sample measurements. At least 4000 gated events were collected for each *S. aureus* sample. Representative histograms for three samples of the negative control and positive control strains of *S. aureus* ATCC 12600 are given in Figure S21. Representative histograms of each strain of *S. aureus* used to characterize the genetic parts and the sensor designs are given in Figures S22−

https://doi.org/10.1021/acssynbio.3c00325
ACS Synth. Biol. 2024, 13, 103−118

S31, grouped by the genetic construct used to characterize the genetic part or the type of genetically encoded sensor.

Constitutive promoters from *B. subtilis* were assayed using the same conditions as that for *S. aureus* with some modifications. First, the cells were grown in M9 minimal medium supplemented with tryptophan. Second, the cells were diluted 160-fold (5 μL of sample media into 195 μL fresh media, twice) after growing for 16 h and after growing for 3 h during the assay. Third, the *B. subtilis* samples were not fixed prior to flow cytometry, and the volumes necessary to dilute the samples for approximately 800−1200 gated events/s differed from *S. aureus*. Finally, at least 6000 gated events were collected for each *B. subtilis* sample.

Fixing *S. aureus* Samples. *S. aureus* samples were fixed using fresh 4% paraformaldehyde in PBS, pH 7−8[91] to kill pathogenic cells prior to flow cytometry and prevent biofilm formation in the flow cytometer. Caution was taken while preparing this solution in a chemical fume hood, as 1 M NaOH and 1 M HCl are highly corrosive, and overheating the paraformaldehyde solution above 65 °C can produce toxic fumes. To make 10 mL of the fixation solution, 0.4 g of powdered paraformaldehyde (Sigma-Aldrich) was added to 7 mL of Milli-Q water in a 50 mL glass beaker, then heated to 60 °C while stirring using a hot plate. After the paraformaldehyde was dissolved, 100 μL of 1 M NaOH was added. One mL of 10× PBS was added after the solution turned clear, and then, the solution was cooled to approximately room temperature while stirring. HCl (100 μL; 1 M) and 1.8 mL of Milli-Q water were added to bring the total volume to 10 mL. The pH was tested at room temperature (MQuant, pH range 2.0−9.0, MilliporeSigma) and adjusted with more 1 M HCl or NaOH solution as needed. The fixation solution was filtered with a 0.22 μm nylon filter (Fisher Scientific) to remove large particles and sterilize the solution before fixing *S. aureus* samples. Note that if the pH of the fixation solution is not adjusted appropriately, the fluorescence of the fixed *S. aureus* samples was greatly affected (Supplemental Note 4 and Figure S32).

After growth for the flow cytometry assay, the 96-well plate of *S. aureus* samples was centrifuged with an aerosol-tight lid at 3900 rpm and room temperature to pellet the cells. The supernatant was then removed by inverting the plate over a large beaker and patting the plate dry on several layers of paper towels to ensure that the supernatant was removed. Next, 200 μL of fixation solution was added to each sample, and the plate was covered and thoroughly sealed with an aluminum seal (Diversified Biotech). The plate was vortexed at 3200 rpm for 30 s to thoroughly mix and resuspend the samples, then incubated at room temperature for 30 min in a fume hood. The samples were then washed three times with sterile PBS by centrifuging the plate with an aerosol-tight lid under the same conditions, removing the supernatant, pipetting 200 μL of sterile PBS into each well, and vortexing the mixture to mix as described above. After three washes, the samples were incubated at room temperature for at least 1 h to allow the fluorescent proteins to fully develop. Finally, samples were mixed by pipetting at least 8 μL up and down 10−20 times before being diluted appropriately into sterile PBS with 2 mg/mL kanamycin for flow cytometry.

Data Analysis. All flow cytometry data were gated in FlowJo (v10.8.0) using a custom FSC-A vs SSC-A gate created for *S. aureus* or *B. subtilis*. These species-specific polygonal gates were created by gating around the wild-type cells and those containing the highly fluorescent reference plasmid (pCM29 for *S. aureus*) or construct (pNH446 for *B. subtilis*) on an FSC-A vs SSC-A plot and then adjusting the gate to minimize the noise (low fluorescence) in the fluorescent samples. All samples were analyzed using the gate appropriate for the species, including samples of *S. aureus* where cells were shifted outside of the gate (SI File 1).

Fluorescent measurements in an experiment used the median FL1-A fluorescence of the gated events. Activity and expression values in *S. aureus* were converted from arbitrary units of fluorescence to relative expression units (REU) using the following equation:

$$\mathrm{REU} = \frac{\mathrm{AU}_{\mathrm{sample}} - \mathrm{AU}_{\mathrm{NC}}}{\mathrm{AU}_{\mathrm{PC}} - \mathrm{AU}_{\mathrm{NC}}}$$

where $\mathrm{AU}_{\mathrm{sample}}$ is the measured fluorescence of the sample, $\mathrm{AU}_{\mathrm{NC}}$ is the measured autofluorescence of the wildtype strain *S. aureus* ATCC 12600 (negative control), and $\mathrm{AU}_{\mathrm{PC}}$ is the measured fluorescence of the *S. aureus* strain containing the pCM29 reference plasmid (positive control). Constitutive promoter activity in *B. subtilis* was converted to relative promoter units (RPU) using the same equation as that for REU with the corresponding negative and positive control strains for *B. subtilis* 168 (wildtype and pNH446 integrated into the genome, respectively). The difference between RPU and REU is the use of an insulated genetic structure (ribozyme, RBS, fluorescent protein coding sequence, terminator) to define the fluorescence of the positive control strain for RPU calculations and to characterize each genetic part.

The average fluorescence of three independent samples (colonies) for the positive and negative controls each was used in the REU or RPU calculation. REU was calculated using a custom Python[92] script (v3.6) and RPU was calculated using Microsoft Excel. Data were imported into RStudio[93] (v1.4.1106) to calculate averages and standard deviations for the three biological replicates of all samples using R (v4.0.4).[94] ggplot2 from the tidyverse package[95] (v1.3.0) was then used to create the graphs of all flow cytometry data. Colors were chosen using colorblind-friendly palettes from the scico package.[96]

The one-way nested ANOVA test for the plasmid replicon data was performed by using the aov() function in *R* with the plasmid replicon factor nested inside the constitutive promoter factor. The Tukey posthoc analysis was performed using the TukeyHSD() function in *R* on the plasmid replicon factor to determine the adjusted *p*-values.

The response function for each sensor design was fit to the Hill equation[97] in the following form:

$$y = y_{\mathrm{min}} + (y_{\mathrm{max}} - y_{\mathrm{min}})\frac{x^n}{K_{\mathrm{d}}^n + x^n}$$

where y is the output activity in REU, x is the input inducer concentration, y_{min} is the minimum (basal) output activity in REU, y_{max} is the maximum output activity in REU, n is the Hill coefficient, and K_{d} is the apparent dissociation constant. For each sensor design, the average output activity in REU at each inducer concentration was transformed onto a $\log_{10}$ scale and then fit to the above Hill equation using the least-squares method to estimate the y_{min}, y_{max}, n, and K_{d} parameters. No upper or lower bounds or initial values for the parameters were applied. The fits were performed using a custom Python script

https://doi.org/10.1021/acssynbio.3c00325
ACS Synth. Biol. 2024, 13, 103−118

and the least_squares() function from SciPy (v1.7.1).[98] Hill parameter values for all sensor designs are given in Table S2.

Constitutive Promoter Alignment. The constitutive promoter sequences from Figure 2A were hand-trimmed from the annotated or predicted transcription start site to the annotated −35 region or 5−10 bp before the predicted −35 region (SI File 1). Because P_{MreB} was not well-annotated, this promoter sequence was trimmed by only two bp at the 5′ end of the sequence. These trimmed promoters were then aligned using the multiple sequence alignment software MAFFT v7.487[59] on a command line using the following options: −maxiterate 1000 −localpair −op 0.75 −ep 3 -reorder. The local alignment (localpair) option was chosen over the global alignment, as the local alignment algorithm provided better alignment for these sequences. The op (gap opening penalty) and ep (offset value, like a gap extension penalty) values were chosen from a matrix of different value combinations until the −35 and −10 regions of most constitutive promoters were aligned as anticipated based on their annotated or predicted sequences.

After alignment, sequence logos of information content (in bits) were created using custom Bash and Python scripts with the Python module Logomaker.[57] Sequence logos of each promoter subset were made by dividing the alignment results from the whole promoter set into each subset. This method was used instead of realigning each promoter subset using the same MAFFT options because the small sample sizes dramatically changed the alignment results. A FASTA file of the alignment results is available in SI File 3.

■ ASSOCIATED CONTENT

Supporting Information

The Supporting Information is available free of charge at https://pubs.acs.org/doi/10.1021/acssynbio.3c00325.

Additional methods used in this work; details on challenges in cloning experiences during this work; experimental details and results for engineering of an IPTG sensor for *S. aureus*; details on cloning plasmids for part characterization; details on the effects of pH of the fixation solution on measured fluorescence of fixed *S. aureus* cells during flow cytometry; characterization of select constitutive promoters using the LAC-p01 replicon; comparison of constitutive promoter activities with and without RiboJ; sequence logos for subsets of constitutive promoters grouped by relative activity measured in *S. aureus* and species of origin; constitutive promoter characterization in *B. subtilis*; multiple sequence alignment of 16S rRNA sequences from *S. aureus* and *B. subtilis*; RBS characterization using P_{SarA1}; comparison of RBS expression between P_{Cap} and P_{SarA1} with and without RiboJ; comparison in ranks of expression for RBSs with and without RiboJ for both P_{Cap} and P_{SarA1}; terminator characterization in REU; plasmid replicon characterization in REU; determination of plasmid copy number in *S. aureus* using qPCR; quantification of growth rates for select strains of *S. aureus*; characterization of an inactive tetracycline sensor design; characterization of IPTG sensor designs; histograms of maximum homology with mismatches of genetic parts in the toolbox against other parts and the *S. aureus* genome; histogram of the lengths of constitutive promoter parts used in this work and Liu et al.; plasmid maps of the plasmid backbones in this work and plasmids used to characterize genetic parts and the sensors; representative histograms of cell fluorescence from flow cytometry data for the negative and positive control strains and strains used to characterize each genetic part and each sensor; representative histograms of the fluorescence from flow cytometry data of the positive and negative controls strains obtained using fixation solutions of different pH; linker sequences used for constructing transcription units in this work; fit Hill equation parameters for each sensor; fit exponential growth rate parameters for select strains of *S. aureus*; description of each plasmid used in this study; sequences of genetic parts used in this work; and sequences and descriptions for DNA oligos used in this study (PDF)

Additional details for each genetic part used in this work; additional details for each plasmid used in this work; trimmed constitutive promoter sequences used for MUSCLE multiple sequence alignment; and detailed checklist of MIQE guidelines for qPCR (XLSX)

SBOL file for each genetic part used in this work (ZIP)

FASTA file of the MUSCLE multiple sequence alignment results (ZIP)

■ AUTHOR INFORMATION

Corresponding Author

Lauren B. Andrews − *Department of Chemical Engineering, Molecular and Cellular Biology Graduate Program, and Biotechnology Training Program, University of Massachusetts Amherst, Amherst, Massachusetts 01003, United States;* orcid.org/0000-0003-1627-1430; Email: lbandrews@umass.edu

Authors

Stephen N. Rondthaler − *Department of Chemical Engineering, University of Massachusetts Amherst, Amherst, Massachusetts 01003, United States*

Biprodev Sarker − *Department of Chemical Engineering, University of Massachusetts Amherst, Amherst, Massachusetts 01003, United States*

Nathaniel Howitz − *Department of Chemical Engineering, University of Massachusetts Amherst, Amherst, Massachusetts 01003, United States*

Ishita Shah − *Department of Chemical Engineering, University of Massachusetts Amherst, Amherst, Massachusetts 01003, United States*

Complete contact information is available at: https://pubs.acs.org/10.1021/acssynbio.3c00325

Author Contributions

S.N.R. and L.B.A conceived the project, designed the experiments, and wrote the manuscript. S.N.R. performed the *S. aureus* experiments. B.S. performed the *B. subtilis* experiments. N.H. and I.S. established the integration plasmid design for *B. subtilis* and designed three *B. subtilis* constitutive promoter sequences (P_{FtsH}, P_{PssA}, P_{TrnQ}). S.N.R. and L.B.A. analyzed the data. L.B.A supervised the research.

Notes

The authors declare no competing financial interest.

https://doi.org/10.1021/acssynbio.3c00325
ACS Synth. Biol. 2024, 13, 103−118

■ ACKNOWLEDGMENTS

This work was supported by funds from the National Science Foundation (DMR-1904901, MCB-2211039, CBET-1943695), a SEED grant from the UMass ADVANCE program (funded by NSF awards 1824090, 2136150), the Marvin and Eva Schlanger faculty fellowship, and startup funds from the University of Massachusetts Amherst to LBA. SNR was supported by a fellowship from the National Science Foundation Graduate Research Fellowship Program (DGE-1451512). We thank Jessica Schiffman for the gift of the pCM29 plasmid. We thank Dr. J. L. Bose for contributing the pKK30 plasmid (NR-50349) distributed by BEI Resources (funded by NIH NIAID) and the Network on Antimicrobial Resistance in *Staphylococcus aureus* (NARSA) for contributing the pCN37 (NR-46126) and pCN56 (NR-46156) plasmids distributed by BEI Resources. We thank the UMass Genomics Resources Laboratory and Sarthak Srivastava and Dominic Castaldi for assistance with qPCR experiments. Finally, we thank current and past members of the Andrews research group and current and past members of Jessica Schiffman's research group for helpful advice.

■ REFERENCES

(1) Khan, H. A.; Ahmad, A.; Mehboob, R. Nosocomial Infections and Their Control Strategies. *Asian Pac. J. Trop. Biomed.* **2015**, *5* (7), 509−514.

(2) Archer, N. K.; Mazaitis, M. J.; Costerton, J. W.; Leid, J. G.; Powers, M. E.; Shirtliff, M. E. Staphylococcus Aureus Biofilms. *Virulence* **2011**, *2* (5), 445−459.

(3) Gahlot, R.; Nigam, C.; Kumar, V.; Yadav, G.; Anupurba, S.; Gahlot, R.; Nigam, C.; Kumar, V.; Yadav, G.; Anupurba, S. Catheter-Related Bloodstream Infections. *Int. J. Crit. Illness Inj. Sci.* **2014**, *4* (2), 162.

(4) Staphylococcus Aureus Infections: Epidemiology, Pathophysiology, Clinical Manifestations, and Management. DOI: DOI: 10.1128/CMR.00134-14.

(5) Kolewe, K. W.; Peyton, S. R.; Schiffman, J. D. Fewer Bacteria Adhere to Softer Hydrogels. *ACS Appl. Mater. Interfaces* **2015**, *7* (35), 19562−19569.

(6) Alam, F.; Balani, K. Adhesion Force of Staphylococcus Aureus on Various Biomaterial Surfaces. *J. Mech. Behav. Biomed. Mater.* **2017**, *65*, 872−880.

(7) Foster, T. J.; Geoghegan, J. A.; Ganesh, V. K.; Höök, M. Adhesion, Invasion and Evasion: The Many Functions of the Surface Proteins of Staphylococcus Aureus. *Nat. Rev. Microbiol* **2014**, *12* (1), 49−62.

(8) Oliveira, D.; Borges, A.; Simões, M. Staphylococcus Aureus Toxins and Their Molecular Activity in Infectious Diseases. *Toxins* **2018**, *10* (6), 252.

(9) Guo, Y.; Song, G.; Sun, M.; Wang, J.; Wang, Y. Prevalence and Therapies of Antibiotic-Resistance in Staphylococcus Aureus. *Front. Cell. Infect. Microbiol.* **2020**, *10*, 107.

(10) Vancomycin Resistant Staphylococcus Aureus Infections: A Review of Case Updating and Clinical Features | Elsevier Enhanced Reader. DOI: DOI: 10.1016/j.jare.2019.10.005.

(11) Bae, T.; Schneewind, O. Allelic Replacement in Staphylococcus Aureus with Inducible Counter-Selection. *Plasmid* **2006**, *55* (1), 58−63.

(12) Blättner, S.; Das, S.; Paprotka, K.; Eilers, U.; Krischke, M.; Kretschmer, D.; Remmele, C. W.; Dittrich, M.; Müller, T.; Schuelein-Voelk, C.; Hertlein, T.; Mueller, M. J.; Huettel, B.; Reinhardt, R.; Ohlsen, K.; Rudel, T.; Fraunholz, M. J. Staphylococcus Aureus Exploits a Non-Ribosomal Cyclic Dipeptide to Modulate Survival within Epithelial Cells and Phagocytes. *PLOS Pathogens* **2016**, *12* (9), No. e1005857.

(13) Weiss, A.; Ibarra, J. A.; Paoletti, J.; Carroll, R. K.; Shaw, L. N. The δ Subunit of RNA Polymerase Guides Promoter Selectivity and Virulence in Staphylococcus Aureus. *Infect. Immun.* **2014**, *82* (4), 1424−1435.

(14) Sargison, F. A.; Fitzgerald, J. R. Advances in Transposon Mutagenesis of Staphylococcus Aureus: Insights into Pathogenesis and Antimicrobial Resistance. *Trends Microbiol.* **2021**, *29* (4), 282−285.

(15) Pang, Y. Y.; Schwartz, J.; Thoendel, M.; Ackermann, L. W.; Horswill, A. R.; Nauseef, W. M. Agr-Dependent Interactions of Staphylococcus Aureus USA300 with Human Polymorphonuclear Neutrophils. *J. Innate Immun.* **2010**, *2* (6), 546−559.

(16) Charpentier, E.; Anton, A. I.; Barry, P.; Alfonso, B.; Fang, Y.; Novick, R. P. Novel Cassette-Based Shuttle Vector System for Gram-Positive Bacteria. *Appl. Environ. Microbiol.* **2004**, *70* (10), 6076−6085.

(17) Schwendener, S.; Perreten, V. New Shuttle Vector-Based Expression System To Generate Polyhistidine-Tagged Fusion Proteins in Staphylococcus Aureus and Escherichia Coli. *Appl. Environ. Microbiol.* **2015**, *81*, 3243.

(18) Malone, C. L.; Boles, B. R.; Lauderdale, K. J.; Thoendel, M.; Kavanaugh, J. S.; Horswill, A. R. Fluorescent Reporters for Staphylococcus Aureus. *J. Microbiol. Methods* **2009**, *77* (3), 251−260.

(19) Zhang, L.; Fan, F.; Palmer, L. M.; Lonetto, M. A.; Petit, C.; Voelker, L. L.; St John, A.; Bankosky, B.; Rosenberg, M.; McDevitt, D. Regulated Gene Expression in Staphylococcus Aureus for Identifying Conditional Lethal Phenotypes and Antibiotic Mode of Action. *Gene* **2000**, *255* (2), 297−305.

(20) Moore, S. J.; Lai, H.-E.; Kelwick, R. J. R.; Chee, S. M.; Bell, D. J.; Polizzi, K. M.; Freemont, P. S. EcoFlex: A Multifunctional MoClo Kit for E. coli Synthetic Biology. *ACS Synth. Biol.* **2016**, *5* (10), 1059−1069.

(21) Iverson, S. V.; Haddock, T. L.; Beal, J.; Densmore, D. M. CIDAR MoClo: Improved MoClo Assembly Standard and New E. Coli Part Library Enable Rapid Combinatorial Design for Synthetic and Traditional Biology. *ACS. Synth. Biol.* **2016**, *5* (1), 99−103.

(22) Kosuri, S.; Goodman, D. B.; Cambray, G.; Mutalik, V. K.; Gao, Y.; Arkin, A. P.; Endy, D.; Church, G. M. Composability of Regulatory Sequences Controlling Transcription and Translation in Escherichia Coli. *Proc. Natl. Acad. Sci. U. S. A.* **2013**, *110* (34), 14024−14029.

(23) Schuster, L. A.; Reisch, C. R. A Plasmid Toolbox for Controlled Gene Expression across the Proteobacteria. *Nucleic Acids Res.* **2021**, *49* (12), 7189−7202.

(24) Bi, C.; Su, P.; Müller, J.; Yeh, Y.-C.; Chhabra, S. R.; Beller, H. R.; Singer, S. W.; Hillson, N. J. Development of a Broad-Host Synthetic Biology Toolbox for Ralstonia Eutropha and Its Application to Engineering Hydrocarbon Biofuel Production. *Microb. Cell Fact.* **2013**, *12* (1), 107.

(25) Mimee, M.; Tucker, A. C.; Voigt, C. A.; Lu, T. K. Programming a Human Commensal Bacterium, Bacteroides Thetaiotaomicron, to Sense and Respond to Stimuli in the Murine Gut Microbiota. *Cell Syst.* **2015**, *1* (1), 62−71.

(26) Markley, A. L.; Begemann, M. B.; Clarke, R. E.; Gordon, G. C.; Pfleger, B. F. Synthetic Biology Toolbox for Controlling Gene Expression in the Cyanobacterium Synechococcus Sp. Strain PCC 7002. *ACS Synth. Biol.* **2015**, *4* (5), 595−603.

(27) Vasudevan, R.; Gale, G. A. R.; Schiavon, A. A.; Puzorjov, A.; Malin, J.; Gillespie, M. D.; Vavitsas, K.; Zulkower, V.; Wang, B.; Howe, C. J.; Lea-Smith, D. J.; McCormick, A. J. CyanoGate: A Modular Cloning Suite for Engineering Cyanobacteria Based on the Plant MoClo Syntax. *Plant Physiol.* **2019**, *180* (1), 39−55.

(28) Guiziou, S.; Sauveplane, V.; Chang, H.-J.; Clerté, C.; Declerck, N.; Jules, M.; Bonnet, J. A Part Toolbox to Tune Genetic Expression in Bacillus Subtilis. *Nucleic Acids Res.* **2016**, *44* (15), 7495−7508.

(29) Radeck, J.; Kraft, K.; Bartels, J.; Cikovic, T.; Dürr, F.; Emenegger, J.; Kelterborn, S.; Sauer, C.; Fritz, G.; Gebhard, S.; Mascher, T. The Bacillus BioBrick Box: Generation and Evaluation of Essential Genetic Building Blocks for Standardized Work with Bacillus Subtilis. *J. Biol. Eng.* **2013**, *7* (1), 29.

(30) Woodruff, L. B. A.; Gorochowski, T. E.; Roehner, N.; Mikkelsen, T. S.; Densmore, D.; Gordon, D. B.; Nicol, R.; Voigt, C. A. Registry in a Tube: Multiplexed Pools of Retrievable Parts for Genetic Design Space Exploration. *Nucleic Acids Res.* **2017**, *45* (3), 1553−1565.
(31) Engler, C.; Kandzia, R.; Marillonnet, S. A One Pot, One Step, Precision Cloning Method with High Throughput Capability. *PLoS One* **2008**, *3* (11), No. e3647.
(32) Potapov, V.; Ong, J. L.; Kucera, R. B.; Langhorst, B. W.; Bilotti, K.; Pryor, J. M.; Cantor, E. J.; Canton, B.; Knight, T. F.; Evans, T. C.; Lohman, G. J. S. Comprehensive Profiling of Four Base Overhang Ligation Fidelity by T4 DNA Ligase and Application to DNA Assembly. *ACS Synth. Biol.* **2018**, *7* (11), 2665−2674.
(33) Pryor, J. M.; Potapov, V.; Kucera, R. B.; Bilotti, K.; Cantor, E. J.; Lohman, G. J. S. Enabling One-Pot Golden Gate Assemblies of Unprecedented Complexity Using Data-Optimized Assembly Design. *PLoS One* **2020**, *15* (9), No. e0238592.
(34) Kelly, J. R.; Rubin, A. J.; Davis, J. H.; Ajo-Franklin, C. M.; Cumbers, J.; Czar, M. J.; de Mora, K.; Glieberman, A. L.; Monie, D. D.; Endy, D. Measuring the Activity of BioBrick Promoters Using an in Vivo Reference Standard. *J. Biol. Eng.* **2009**, *3* (1), 4.
(35) Nielsen, A. A. K.; Der, B. S.; Shin, J.; Vaidyanathan, P.; Paralanov, V.; Strychalski, E. A.; Ross, D.; Densmore, D.; Voigt, C. A. Genetic Circuit Design Automation. *Science* **2016**, *352* (6281), No. aac7341.
(36) Reis, A. C.; Salis, H. M. An Automated Model Test System for Systematic Development and Improvement of Gene Expression Models. *ACS Synth. Biol.* **2020**, *9* (11), 3145−3156.
(37) Espah Borujeni, A.; Salis, H. M. Translation Initiation Is Controlled by RNA Folding Kinetics via a Ribosome Drafting Mechanism. *J. Am. Chem. Soc.* **2016**, *138* (22), 7016−7023.
(38) Espah Borujeni, A.; Channarasappa, A. S.; Salis, H. M. Translation Rate Is Controlled by Coupled Trade-Offs between Site Accessibility, Selective RNA Unfolding and Sliding at Upstream Standby Sites. *Nucleic Acids Res.* **2014**, *42* (4), 2646−2659.
(39) Espah Borujeni, A.; Cetnar, D.; Farasat, I.; Smith, A.; Lundgren, N.; Salis, H. M. Precise Quantification of Translation Inhibition by MRNA Structures That Overlap with the Ribosomal Footprint in N-Terminal Coding Sequences. *Nucleic Acids Res.* **2017**, *45* (9), 5437−5448.
(40) Crosby, H. A.; Schlievert, P. M.; Merriman, J. A.; King, J. M.; Salgado-Pabón, W.; Horswill, A. R. The Staphylococcus Aureus Global Regulator MgrA Modulates Clumping and Virulence by Controlling Surface Protein Expression. *PLOS Pathogens* **2016**, *12* (5), No. e1005604.
(41) Gao, P.; Wang, Y.; Villanueva, I.; Ho, P. L.; Davies, J.; Kao, R. Y. T. Construction of a Multiplex Promoter Reporter Platform to Monitor Staphylococcus Aureus Virulence Gene Expression and the Identification of Usnic Acid as a Potent Suppressor of Psm Gene Expression. *Front. Microbiol.* **2016**, *7*, No. 01344.
(42) Liu, Q.; Li, D.; Wang, N.; Guo, G.; Shi, Y.; Zou, Q.; Zhang, X. Identification and Application of a Panel of Constitutive Promoters for Gene Overexpression in Staphylococcus Aureus. *Front. Microbiol.* **2022**, *13*, 818307.
(43) McLaughlin, J. R.; Murray, C. L.; Rabinowitz, J. C. Unique Features in the Ribosome Binding Site Sequence of the Gram-Positive Staphylococcus Aureus Beta-Lactamase Gene. *J. Biol. Chem.* **1981**, *256* (21), 11283−11291.
(44) Ballal, A.; Manna, A. C. Regulation of Superoxide Dismutase (Sod) Genes by SarA in Staphylococcus Aureus. *J. Bacteriol.* **2009**, *191*, 3301.
(45) Bayer, M. G.; Heinrichs, J. H.; Cheung, A. L. The Molecular Architecture of the Sar Locus in Staphylococcus Aureus. *J. Bacteriol.* **1996**, *178*, 4563.
(46) Liu, Q.; Yeo, W.-S.; Bae, T. The SaeRS Two-Component System of Staphylococcus Aureus. *Genes* **2016**, *7* (10), 81.
(47) Ouyang, S.; Lee, C. Y. Transcriptional Analysis of Type 1 Capsule Genes in Staphylococcus Aureus. *Mol. Microbiol.* **1997**, *23* (3), 473−482.
(48) Song, Y.; Nikoloff, J. M.; Fu, G.; Chen, J.; Li, Q.; Xie, N.; Zheng, P.; Sun, J.; Zhang, D. Promoter Screening from Bacillus Subtilis in Various Conditions Hunting for Synthetic Biology and Industrial Applications. *PLoS One* **2016**, *11* (7), No. e0158447.
(49) Voskuil, M. The −16 Region of Bacillus Subtilis and Other Gram-Positive Bacterial Promoters. *Nucleic Acids Res.* **1998**, *26* (15), 3584−3590.
(50) Lu, Z.; Yang, S.; Yuan, X.; Shi, Y.; Ouyang, L.; Jiang, S.; Yi, L.; Zhang, G. CRISPR-Assisted Multi-Dimensional Regulation for Fine-Tuning Gene Expression in Bacillus Subtilis. *Nucleic Acids Res.* **2019**, *47* (7), No. e40.
(51) Krasny, L.; Gourse, R. L. An Alternative Strategy for Bacterial Ribosome Synthesis: Bacillus Subtilis RRNA Transcription Regulation. *EMBO J.* **2004**, *23* (22), 4473−4483.
(52) Wetzstein, M.; Völker, U.; Dedio, J.; Löbau, S.; Zuber, U.; Schiesswohl, M.; Herget, C.; Hecker, M.; Schumann, W. Cloning, Sequencing, and Molecular Analysis of the DnaK Locus from Bacillus Subtilis. *J. Bacteriol.* **1992**, *174*, 3300.
(53) Mirouze, N.; Ferret, C.; Yao, Z.; Chastanet, A.; Carballido-López, R. MreB-Dependent Inhibition of Cell Elongation during the Escape from Competence in Bacillus Subtilis. *PLOS Genet.* **2015**, *11* (6), No. e1005299.
(54) Ludwig, H.; Homuth, G.; Schmalisch, M.; Dyka, F. M.; Hecker, M.; Stülke, J. Transcription of Glycolytic Genes and Operons in Bacillus Subtilis: Evidence for the Presence of Multiple Levels of Control of the GapA Operon. *Mol. Microbiol.* **2001**, *41* (2), 409−422.
(55) Micka, B.; Groch, N.; Heinemann, U.; Marahiel, M. A. Molecular Cloning, Nucleotide Sequence, and Characterization of the Bacillus Subtilis Gene Encoding the DNA-Binding Protein HBsu. *J. Bacteriol.* **1991**, *173*, 3191.
(56) Deora, R.; Misra, T. K. Characterization of the Primary σ Factor of Staphylococcus Aureus. *J. Biol. Chem.* **1996**, *271* (36), 21828−21834.
(57) Tareen, A.; Kinney, J. B. Logomaker: Beautiful Sequence Logos in Python. *Bioinformatics* **2020**, *36* (7), 2272−2274.
(58) Lou, C.; Stanton, B.; Chen, Y.-J.; Munsky, B.; Voigt, C. A. Ribozyme-Based Insulator Parts Buffer Synthetic Circuits from Genetic Context. *Nat. Biotechnol.* **2012**, *30* (11), 1137−1142.
(59) Katoh, K.; Standley, D. M. MAFFT Multiple Sequence Alignment Software Version 7: Improvements in Performance and Usability. *Mol. Biol. Evol.* **2013**, *30* (4), 772−780.
(60) Cheng, J.; Guan, C.; Cui, W.; Zhou, L.; Liu, Z.; Li, W.; Zhou, Z. Enhancement of a High Efficient Autoinducible Expression System in Bacillus Subtilis by Promoter Engineering. *Protein Expression Purif.* **2016**, *127*, 81−87.
(61) Guan, C.; Cui, W.; Cheng, J.; Zhou, L.; Liu, Z.; Zhou, Z. Development of an Efficient Autoinducible Expression System by Promoter Engineering in Bacillus Subtilis. *Microb. Cell Fact.* **2016**, *15* (1), 66.
(62) Clifton, K. P.; Jones, E. M.; Paudel, S.; Marken, J. P.; Monette, C. E.; Halleran, A. D.; Epp, L.; Saha, M. S. The Genetic Insulator RiboJ Increases Expression of Insulated Genes. *J. Biol. Eng.* **2018**, *12* (1), 23.
(63) Chen, Y.-J.; Liu, P.; Nielsen, A. A. K.; Brophy, J. A. N.; Clancy, K.; Peterson, T.; Voigt, C. A. Characterization of 582 Natural and Synthetic Terminators and Quantification of Their Design Constraints. *Nat. Methods* **2013**, *10* (7), 659−664.
(64) Cambray, G.; Guimaraes, J. C.; Mutalik, V. K.; Lam, C.; Mai, Q.-A.; Thimmaiah, T.; Carothers, J. M.; Arkin, A. P.; Endy, D. Measurement and Modeling of Intrinsic Transcription Terminators. *Nucleic Acids Res.* **2013**, *41* (9), 5139−5148.
(65) Krute, C. N.; Krausz, K. L.; Markiewicz, M. A.; Joyner, J. A.; Pokhrel, S.; Hall, P. R.; Bose, J. L. Generation of a Stable Plasmid for In Vitro and In Vivo Studies of Staphylococcus Species. *Appl. Environ. Microbiol.* **2016**, *82*, 6859.
(66) Novick, R. P. [27] Genetic Systems in Staphylococci. In *Methods in Enzymology; Bacterial Genetic Systems*; Academic Press, 1991; Vol. *204*, pp 587−636.

https://doi.org/10.1021/acssynbio.3c00325
ACS Synth. Biol. 2024, 13, 103−118

(67) Wang, B.; Barahona, M.; Buck, M. Amplification of Small Molecule-Inducible Gene Expression via Tuning of Intracellular Receptor Densities. *Nucleic Acids Res.* **2015**, *43* (3), 1955−1964.
(68) Brewster, R. C.; Weinert, F. M.; Garcia, H. G.; Song, D.; Rydenfelt, M.; Phillips, R. The Transcription Factor Titration Effect Dictates Level of Gene Expression. *Cell* **2014**, *156* (6), 1312−1323.
(69) Corrigan, R. M.; Foster, T. J. An Improved Tetracycline-Inducible Expression Vector for Staphylococcus Aureus. *Plasmid* **2009**, *61* (2), 126−129.
(70) Brzoska, A. J.; Firth, N. Two-Plasmid Vector System for Independently Controlled Expression of Green and Red Fluorescent Fusion Proteins in Staphylococcus Aureus. *Appl. Environ. Microbiol.* **2013**, *79*, 3133.
(71) Bateman, B. T.; Donegan, N. P.; Jarry, T. M.; Palma, M.; Cheung, A. L. Evaluation of a Tetracycline-Inducible Promoter InStaphylococcus Aureus In Vitro and In Vivo and Its Application in Demonstrating the Role of SigB in Microcolony Formation. *Infect. Immun.* **2001**, *69* (12), 7851−7857.
(72) Jack, B. R.; Leonard, S. P.; Mishler, D. M.; Renda, B. A.; Leon, D.; Suárez, G. A.; Barrick, J. E. Predicting the Genetic Stability of Engineered DNA Sequences with the EFM Calculator. *ACS Synth. Biol.* **2015**, *4* (8), 939−943.
(73) Shen, P.; Huang, H. V. Homologous Recombination in ESCHERICHIA COLI: Dependence on Substrate Length and Homology. *Genetics* **1986**, *112* (3), 441−457.
(74) LaFleur, T. L.; Hossain, A.; Salis, H. M. Automated Model-Predictive Design of Synthetic Promoters to Control Transcriptional Profiles in Bacteria. *Nat. Commun.* **2022**, *13* (1), 5159.
(75) Wang, Y.; Wang, H.; Wei, L.; Li, S.; Liu, L.; Wang, X. Synthetic Promoter Design in Escherichia Coli Based on a Deep Generative Network. *Nucleic Acids Res.* **2020**, *48* (12), 6403−6412.
(76) Rohlhill, J.; Sandoval, N. R.; Papoutsakis, E. T. Sort-Seq Approach to Engineering a Formaldehyde-Inducible Promoter for Dynamically Regulated Escherichia Coli Growth on Methanol. *ACS Synth. Biol.* **2017**, *6* (8), 1584−1595.
(77) Levy, L.; Anavy, L.; Solomon, O.; Cohen, R.; Brunwasser-Meirom, M.; Ohayon, S.; Atar, O.; Goldberg, S.; Yakhini, Z.; Amit, R. A Synthetic Oligo Library and Sequencing Approach Reveals an Insulation Mechanism Encoded within Bacterial Σ54 Promoters. *Cell Rep.* **2017**, *21* (3), 845−858.
(78) Liu, C.; Zhang, B.; Liu, Y.-M.; Yang, K.-Q.; Liu, S.-J. New Intracellular Shikimic Acid Biosensor for Monitoring Shikimate Synthesis in Corynebacterium Glutamicum. *ACS Synth. Biol.* **2018**, *7* (2), 591−601.
(79) Geissendörfer, M.; Hillen, W. Regulated Expression of Heterologous Genes in Bacillus Subtilis Using the Tn10 Encoded Tet Regulatory Elements. *Appl. Microbiol. Biotechnol.* **1990**, *33* (6), 657−663.
(80) Yansura, D. G.; Henner, D. J. Use of the Escherichia Coli Lac Repressor and Operator to Control Gene Expression in Bacillus Subtilis. *Proc. Natl. Acad. Sci. U. S. A.* **1984**, *81* (2), 439−443.
(81) Johns, N. I.; Gomes, A. L. C.; Yim, S. S.; Yang, A.; Blazejewski, T.; Smillie, C. S.; Smith, M. B.; Alm, E. J.; Kosuri, S.; Wang, H. H. Metagenomic Mining of Regulatory Elements Enables Programmable Species-Selective Gene Expression. *Nat. Methods* **2018**, *15* (5), 323−329.
(82) Bose, J. L.; Fey, P. D.; Bayles, K. W. Genetic Tools To Enhance the Study of Gene Function and Regulation in Staphylococcus Aureus. *Appl. Environ. Microbiol.* **2013**, *79* (7), 2218−2224.
(83) Penewit, K.; Holmes, E. A.; McLean, K.; Ren, M.; Waalkes, A.; Salipante, S. J. Efficient and Scalable Precision Genome Editing in Staphylococcus Aureus through Conditional Recombineering and CRISPR/Cas9-Mediated Counterselection. *mBio* **2018**, *9* (1), No. e00067-18.
(84) Gruss, A.; Ehrlich, S. D. Insertion of Foreign DNA into Plasmids from Gram-Positive Bacteria Induces Formation of High-Molecular-Weight Plasmid Multimers. *J. Bacteriol.* **1988**, *170* (3), 1183−1190.
(85) Grkovic, S.; Brown, M. H.; Hardie, K. M.; Firth, N.; Skurray, R. A. Stable Low-Copy-Number Staphylococcus Aureus Shuttle Vectors. *Microbiology* **2003**, *149* (3), 785−794.
(86) Firth, N.; Apisiridej, S.; Berg, T.; O'Rourke, B. A.; Curnock, S.; Dyke, K. G. H.; Skurray, R. A. Replication of Staphylococcal Multiresistance Plasmids. *J. Bacteriol.* **2000**, *182* (8), 2170−2178.
(87) Monk, I. R.; Tree, J. J.; Howden, B. P.; Stinear, T. P.; Foster, T. J. Complete Bypass of Restriction Systems for Major Staphylococcus Aureus Lineages. *mBio* **2015**, *6*, No. e00308-15, DOI: 10.1128/mBio.00308-15.
(88) Reed, P.; Atilano, M. L.; Alves, R.; Hoiczyk, E.; Sher, X.; Reichmann, N. T.; Pereira, P. M.; Roemer, T.; Filipe, S. R.; Pereira-Leal, J. B.; Ligoxygakis, P.; Pinho, M. G. Staphylococcus Aureus Survives with a Minimal Peptidoglycan Synthesis Machine but Sacrifices Virulence and Antibiotic Resistance. *PLOS Pathog.* **2015**, *11* (5), No. e1004891.
(89) Schenk, S.; Laddaga, R. A. Improved Method for Electroporation of Staphylococcus Aureus. *FEMS Microbiol. Lett.* **1992**, *94* (1−2), 133−138.
(90) Löfblom, J.; Kronqvist, N.; Uhlén, M.; Ståhl, S.; Wernérus, H. Optimization of Electroporation-Mediated Transformation: Staphylococcus Carnosus as Model Organism. *J. Appl. Microbiol.* **2007**, *102* (3), 736−747.
(91) Paraformaldehyde in PBS. *Cold Spring Harb. Protoc.* **2006**, *2006* (1), pdb.rec9959.
(92) Van Rossum, G.; Drake, F. L. *Python 3 Reference Manual*; CreateSpace: Scotts Valley, CA, 2009.
(93) RStudio *Open source & professional software for data science teams*. https://rstudio.com/ (accessed January 3, 2022).
(94) R Core Team. *R: A Language and Environment for Statistical Computing*; R Foundation for Statistical Computing: Vienna, Austria, 2021.
(95) Wickham, H.; Averick, M.; Bryan, J.; Chang, W.; McGowan, L. D.; François, R.; Grolemund, G.; Hayes, A.; Henry, L.; Hester, J.; Kuhn, M.; Pedersen, T. L.; Miller, E.; Bache, S. M.; Müller, K.; Ooms, J.; Robinson, D.; Seidel, D. P.; Spinu, V.; Takahashi, K.; Vaughan, D.; Wilke, C.; Woo, K.; Yutani, H. Welcome to the Tidyverse. *J. Open Source Software* **2019**, *4* (43), 1686.
(96) Crameri, F.; Shephard, G. E.; Heron, P. J. The Misuse of Colour in Science Communication. *Nat. Commun.* **2020**, *11* (1), 5444.
(97) Ang, J.; Harris, E.; Hussey, B. J.; Kil, R.; McMillen, D. R. Tuning Response Curves for Synthetic Biology. *ACS Synth. Biol.* **2013**, *2* (10), 547−567.
(98) Virtanen, P.; Gommers, R.; Oliphant, T. E.; Haberland, M.; Reddy, T.; Cournapeau, D.; Burovski, E.; Peterson, P.; Weckesser, W.; Bright, J.; van der Walt, S. J.; Brett, M.; Wilson, J.; Millman, K. J.; Mayorov, N.; Nelson, A. R. J.; Jones, E.; Kern, R.; Larson, E.; Carey, C. J.; Polat, İ.; Feng, Y.; Moore, E. W.; VanderPlas, J.; Laxalde, D.; Perktold, J.; Cimrman, R.; Henriksen, I.; Quintero, E. A.; Harris, C. R.; Archibald, A. M.; Ribeiro, A. H.; Pedregosa, F.; van Mulbregt, P. SciPy 1.0: Fundamental Algorithms for Scientific Computing in Python. *Nat. Methods* **2020**, *17* (3), 261−272.